Title

Cardio-audio synchronization elicits prediction in auditory sequences during human wakefulness and sleep

Authors

Andria Pelentritou[1*], Christian Pfeiffer[2], Sophie Schwartz[3] & Marzia De Lucia[1*]

Affiliations

[1]Laboratoire de Recherche en Neuroimagerie (LREN), University Hospital (CHUV) and University of Lausanne (UNIL), Lausanne, Switzerland

[2]Robotics and Perception Group, University of Zurich, Zurich, Switzerland

[3]Department of Neuroscience, Faculty of Medicine & Swiss Center for Affective Sciences & Geneva Neuroscience Center, University of Geneva, Geneva, Switzerland

Contact info

Correspondence: Antria.Pelentritou@chuv.ch, Marzia.De-Lucia@chuv.ch.

Summary

The human brain can infer temporal regularities across cardiac and auditory inputs. Here, we investigated whether cardio-audio regularity processing occurs during sleep, when the balance between bodily and environmental stimulus processing may be altered. Using electroencephalography and electrocardiography in healthy volunteers (N=26) during wakefulness and sleep, we measured the response to unexpected sound omissions within three regularity conditions: synchronous, where sound and heartbeat are temporally coupled, isochronous, with fixed sound-to-sound intervals, and a third control condition without specific regularity. The synchronous and isochronous sequences induced a modulation of the omission-evoked neural response in wakefulness and N2 sleep, the latter accompanied by a reorganization of the background oscillatory activity. Cardio-audio regularity encoding was further demonstrated by a heartbeat deceleration upon omissions in all vigilance states, higher in the synchronous compared to the other regularity types. The human brain processes cardio-audio temporal relationships to predict future auditory events across distinct vigilance stages.

Keywords

Sleep, Electroencephalography, Electrocardiography, Auditory Processing, Interoceptive Processing, Statistical Learning, Predictive Coding, Omission Response, Heartbeat Evoked Response

Introduction

The human brain capitalizes on learning the statistical temporal structure of incoming sensory inputs to inform future sensory experiences. Sensitivity to auditory regularities can manifest as a differential neural response to deviant stimuli in comparison to frequently repeated sounds, often referred to as mismatch negativity (MMN) in electroencephalographic (EEG) studies (Garrido et al., 2009). This rudimental component of auditory discrimination has often been interpreted in the framework of the predictive coding theory (Barascud et al., 2016; Garrido et al., 2008; Heilbron and Chait, 2018; Näätänen et al., 2007; Todorovic et al., 2011). According to this theory, the MMN may arise from the contribution of multiple, non-exclusive mechanisms including repetition suppression in response to frequent stimuli and generation of a 'prediction error' following an unexpected mismatch between the predicted and presented stimuli. The predictive nature of the neural responses to violations within regular auditory sequences has received experimental support from studies on unexpected omissions (Chennu et al., 2016; Demarchi et al., 2019; Recasens and Uhlhaas, 2017; SanMiguel et al., 2013a; Wacongne et al., 2011) where the top-down prediction is not confounded by the neural response to deviant sound stimuli.

Recent studies demonstrated that auditory prediction is not limited to fixed sound-to-sound regularities, but it extends to pseudo-regular sequences in which temporal prediction is induced by locking the sound onsets to interoceptive inputs, *i.e.* internally-generated signals such as the heartbeat. Van Elk and colleagues (2014) revealed a modulation of the auditory event-related potential by the ongoing cardiac input, wherein the auditory N100 was reduced when sounds occurred at a fixed delay relative to the heartbeat signal, compared to when they bared no relationship to the heartbeat (Van Elk et al., 2014). Pfeiffer and De Lucia (2017) reported a greater surprise response during sound omissions, when sound presentations were temporally locked to the ongoing heartbeat as compared to sound presentations unrelated to the ongoing heartbeat (Pfeiffer and De Lucia, 2017). Consistent with the interpretation of the omission response in terms of prediction error, unexpected sound omissions within cardio-audio regularities elicited an enhanced response when participants paid attention to their ongoing heartbeat (Banellis and Cruse, 2020). Taken together, these studies suggest that auditory stimulus expectation is informed by the interoceptive heartbeat signals, thus modulating prediction errors upon deviants from regular auditory sequences.

To date, it remains unknown whether interoceptive signals similarly affect exteroceptive signal processing during sleep, when consciousness or attentional levels are altered, and perception of the external environment is reduced compared to wakefulness. Moreover, auditory regularity processing investigation in sleep has so far been limited to classic MMN responses - *e.g.* in NREM sleep (Sabri et al., 2002, 2003; Winter et al., 1995) and in REM sleep (Sculthorpe et al., 2009) - while no studies - to the best of our knowledge - have documented classic omission responses during sleep. Upon consideration of the implicit nature of the prediction error generation (Lecaignard et al., 2015; Pfeiffer

and De Lucia, 2017), we hypothesised that violation detection signals would be observed during both wakefulness and sleep. In addition, since bodily signals are processed across vigilance states (Lechinger et al., 2015; Perogamvros et al., 2019), we expected that auditory regularity processing during sleep extends to inferences based on the temporal coupling between auditory and cardiac inputs. To test the above hypotheses, healthy volunteers underwent two separate sessions of simultaneous EEG and electrocardiography (ECG) recordings during wakefulness and full night sleep. Participants passively listened to series of sounds forming three possible types of sequences or conditions. In the first condition, sounds were presented with a fixed delay relative to the ongoing heartbeat (synchronous or synch condition), in the second, the sounds followed a fixed sound-to-sound interval (isochronous or isoch condition) and in the third condition, sounds were presented without any temporal regularity relative to heartbeats or to preceding sounds (asynchronous or asynch condition). Upon sound omissions in sleep and wakefulness, we expected prediction error generation in the synch and isoch conditions driven by cardio-audio regularity and temporal auditory regularity, respectively, but not in the asynch condition where no temporal integration between cardiac and/or auditory signals could be performed.

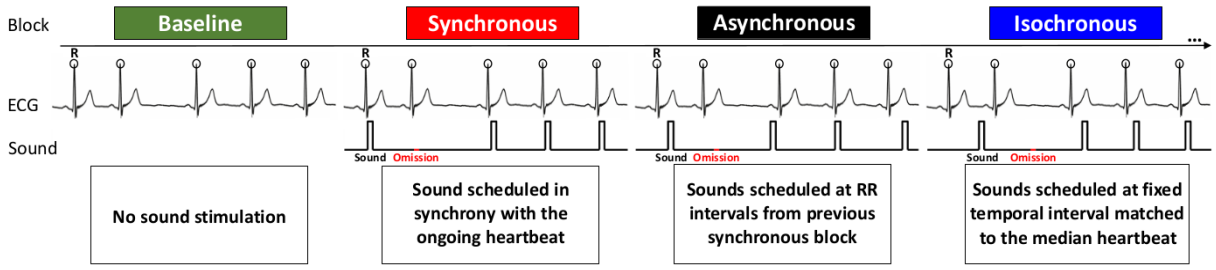

Figure 1. Experimental paradigm overview. The data acquisition was organized in four block types, administered in pseudo-random order. No auditory stimulation was performed during the Baseline condition. In the Synchronous condition, the R peaks (circles) were detected online in the ECG signal and the sounds were administered at a fixed 50 ms R-to-sound and variable sound-to-sound interval. In the Asynchronous condition, sound-to-sound intervals from a preceding Synchronous blocks were administered resulting in variable R-to-sound and sound-to-sound intervals. In the Isochronous condition, the median interbeat interval from a preceding Synchronous block was computed and served as the fixed sound-to-sound interval. Sound omissions occurred pseudo-randomly for 20% of trials within each block.

Results

1. Subject Demographics and Sleep Characteristics

1.1. Participants

Twenty-six healthy volunteers participated in the study (14 female; 1 left-handed; mean age: 27 years, range: 20-35 years) and each took part in a wakefulness and sleep recording session. All 26 participants were included for wakefulness while the sleep dataset included 25 participants (13 female; 1 left-handed;

mean age: 26 years, range: 20-35 years) due to malfunctioning equipment during the sleep session for one participant.

We performed the analyses of the simultaneously acquired EEG and ECG signals. For the EEG analysis, the data of 5 participants were excluded for the wakefulness session due to excessive artifactual periods during acquisition (which yielded a loss of more than 50% of the trials), resulting in the inclusion of 21 out of 26 participants. For the sleep session, from 25 participants, we included 13 participants for N1, 23 participants for N2, 14 for N3, and 13 for REM sleep. For the ECG analysis, we included all 26 participants for the wakefulness session and 18 participants for N1 sleep, 24 participants for N2 sleep, 18 participants for N3 sleep, and 17 participants for REM sleep (*Suppl. Tables 1 & 2*).

1.2. Sleep Characteristics

The sleep characteristics recorded during the experimental night across the eligible population (N=25) are summarized in *Table 1*.

Table 1. Group averaged sleep characteristics (N=25). Total Bed Time calculated based on Lights Off and Lights On time points. Total Sleep Time computed as the period between the Sleep Onset, uncovered by the sleep staging and including possible arousal periods during the night. Percentages of awake periods (AWAKE) and sleep stages (N1, N2, N3, REM) during the session were computed in relation to the Total Bed Time. Sleep efficiency (%) = Total Sleep Time/Total Bed Time for each participant×100. SD=Standard Deviation.

N=25	**Mean**	**SD**
Total Bed Time (min)	420.3	93.8
Total Sleep Time (min)	302.4	107.9
Sleep Efficiency (%)	69.8	12.9
Sleep Onset (min)	24.6	19.1
AWAKE (%)	26.8	12.7
N1 (%)	8.4	2.2
N2 (%)	40.2	9.1
N3 (%)	11.4	5.4
REM (%)	12.1	3.9

2. Quality Control Analysis

We conducted a series of control analyses on the heart rate and the relation between heartbeat and sound onsets across the auditory conditions in order to identify possible factors influencing the neural response to sound omissions during the wakefulness and sleep sessions. In the following, we will refer to R as the latency of the R peak of the ECG waveform (*Figure 1*), S represents the sound onset latency, RR the R peak to R peak latency, SS the sound-to-sound latency, RS the R peak-to-sound latency, SR the sound to the next R peak latency, and variability is calculated as the standard error of the mean (SEM). One way repeated measures analyses of variance (ANOVAs) with factor Condition (synch, asynch, isoch,

baseline where relevant) were performed on the group RR interval, RR variability, SS interval, SS variability, RS interval and RS variability for sound trials, as well as SR interval and SR variability for omission trials (*Suppl. Figure 1*).

By construction, we expected lower RS variability in the synch relative to the two other conditions (isoch and asynch), as was confirmed by one way repeated measures ANOVAs with factor Auditory Condition (synch, asynch, isoch) (*Suppl. Figure 1b*; AWAKE: $F_{(1,3)}$=885.7, p<0.0005; N1: $F_{(1,3)}$=172.5, p<0.0005; N2: $F_{(1,3)}$=230.3, p<0.0005; N3: $F_{(1,3)}$=141.4, p<0.0005; REM: $F_{(1,3)}$=122.1, p<0.0005; all post-hoc t-tests demonstrated lower variability (p<0.0005) in the synch compared to the asynch or isoch condition). In addition, as expected, SR within omission was more variable in the asynch and isoch conditions compared to the synch condition (*Suppl. Figure 1d*; AWAKE: $F_{(1,3)}$=648.5, p<0.0005; N1: $F_{(1,3)}$=77.0, p<0.0005; N2: $F_{(1,3)}$=223.4, p<0.0005; N3: $F(_{(1,3)}$=66.4, p<0.0005; REM: $F_{(1,3)}$=83.7; p<0.0005; post-hoc pairwise comparisons confirmed significantly higher intervals (p<0.0005)). The analysis of the auditory regularity based on the SS onset confirmed higher variability during the synch and asynch compared to the isoch condition (*Suppl. Figure 1f*; AWAKE: $F_{(1,3)}$=58.1, p<0.0005; N1: $F_{(1,3)}$=17.5, p<0.0005; N2: $F_{(1,3)}$=24.1, p<0.0005; N3: $F_{(1,3)}$=12.2, p<0.0005; REM: $F_{(1,3)}$=17.7, p<0.0005; pairwise t-tests (p<0.0005)). During the sleep session, the heartbeat was not globally affected by the different cardio-audio and audio-audio stimulus presentation conditions as shown by 1x4 repeated measures ANOVAs on average RR intervals with factor Condition (synch, asynch, isoch, baseline) (*Suppl. Figure 1g*; N1: $F_{(1,4)}$=2.1, p>0.05; N2: $F_{(1,4)}$=2.4, p>0.05; N3: $F_{(1,4)}$=1.8, p>0.05; REM: $F_{(1,4)}$=0.2, p>0.05). Conversely, the same analysis performed in wakefulness revealed significant differences in RR intervals (*Suppl. Figure 1g*; $F_{(1,4)}$=10.3, p<0.0005). Post-hoc pairwise t-tests uncovered that significantly reduced RR intervals were specific to the baseline condition (synch versus baseline, asynch versus baseline, isoch versus baseline, all p<0.005) while no differences were observed across auditory conditions (p>0.05).

Finally, we performed a control analysis on the ECG waveforms to exclude the potential confound in the interpretation of the differential EEG signals locked to the R peak across conditions of interest due to a possible different degree of contamination of the ECG artifacts into the EEG between conditions of interest. To this aim, we performed a time-wise ECG waveform (for ECG trials time-locked to R peaks during sound omissions) statistical analysis using 1x4 repeated measures ANOVAs with factor Condition (synch, asynch, isoch, baseline) and a False Discovery Rate procedure (Benjamini and Hochberg, 1995) to correct for multiple comparisons across time. No significant differences between the synch, asynch, isoch and baseline conditions were observed for any of the sleep stages (N1: $F_{(1,4)}$=1.2, p>0.05; N2: $F_{(1,4)}$=0.9, p>0.05; N3: $F_{(1,4)}$=0.7, p>0.05; REM: $F_{(1,4)}$=0., p>0.05, averaged F values across time-points). In wakefulness, the ANOVA results on the group averaged ECG waveforms revealed a significant main effect of Condition ($F_{(1,4)}$=3.1, p<0.05). Post-hoc paired t-tests showed that no differences existed between the ECG waveform of the synch and asynch conditions while significant

differences were observed in the synch to baseline time-wise comparison at -99 ms to -28 ms, 23 ms to 53 ms, 280 ms to 294 ms, 365 ms to 466 ms and in the asynch to baseline time-wise comparison at -95 ms to -27 ms, 27 ms to 53 ms, 368 ms to 443 ms.

3. Neural Omission Response

3.1. Auditory evoked potentials

Auditory evoked potentials (AEPs) were computed as the average of the peri-stimulus EEG epochs between 100 ms pre-stimulus and 500 ms post-stimulus onset in the synch, asynch and isoch conditions for the wakefulness session and all sleep stages, in order to qualitatively assess the outcome of the auditory stimulation procedure. The AEPs revealed the expected event-related potential components including the N100 at approximately 100 ms post-stimulus onset and similar AEP morphologies across sleep stages provided qualitative evidence that sound stimuli were processed by the participant's brain (*Figure 2*).

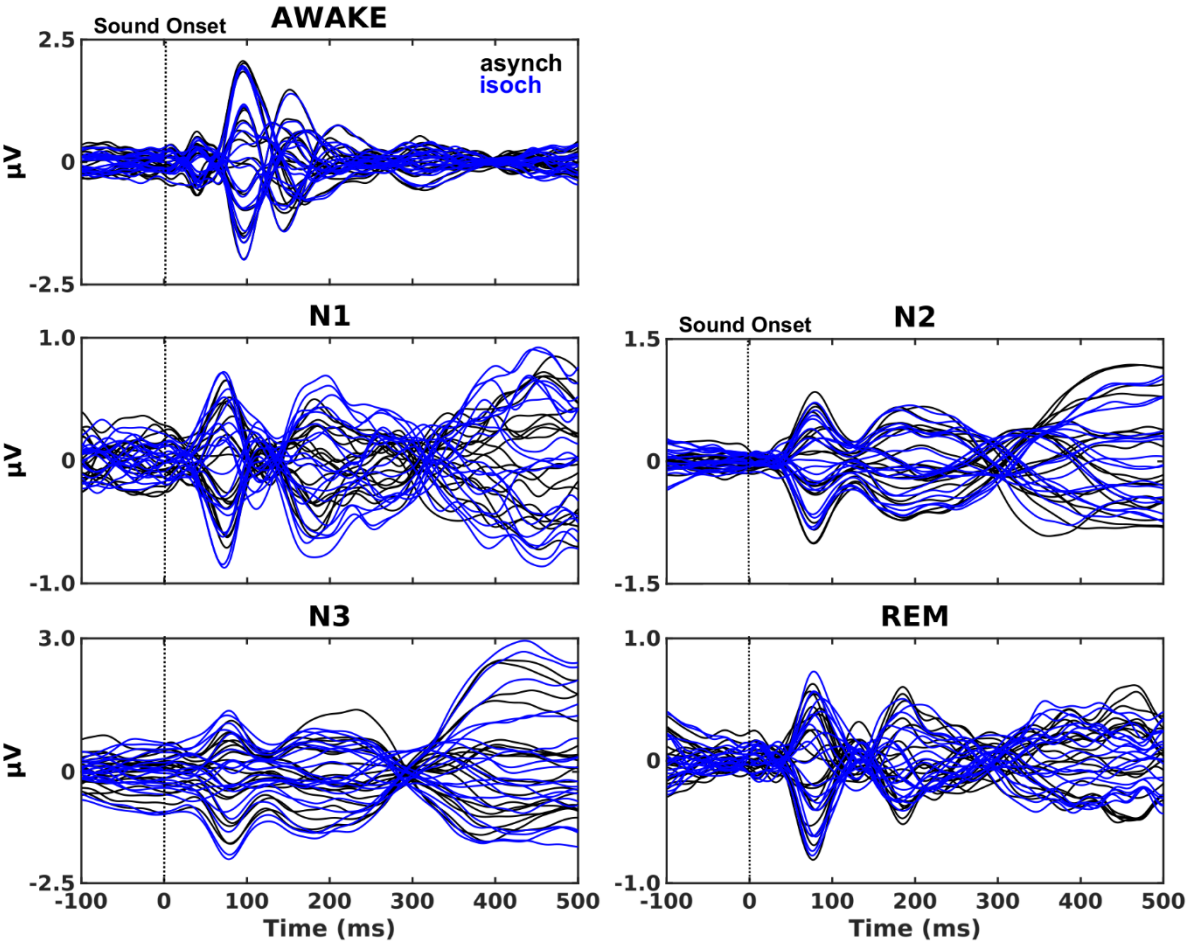

Figure 2. AEPs in wakefulness and sleep. Grand averaged AEPs (time-locked to sound onset) in the isoch (blue lines) and asynch (black lines) across 19 EEG sensors (10-20 system; for visualization purposes) in the wakefulness session (AWAKE) and all stages of sleep (N1, N2, N3, REM). AEPs in wakefulness display the expected electrophysiological signatures, for example, the N100 as the first and highest in amplitude component.

AEPs are also observed in all sleep stages, yet with differences in signal morphology, signal amplitude, and latency of the response. Note that the AEPs of the synch condition are not depicted as they would be superimposed with the heartbeat evoked potential.

3.2. Heartbeat-based omission response

To investigate the effect of cardio-audio synchronicity on omission responses, we derived heartbeat-evoked potentials (HEPs) during sound omissions in the synch and asynch conditions in wakefulness and all sleep stages (AWAKE: N=21; N1: N=13; N2: N=23; N3: N=14; REM: N=13). Average omission HEPs were calculated by extracting epochs from the continuous EEG recordings that were time-locked to the first R peak of the ECG signal during omissions. As an additional control condition for this analysis, we extracted a random selection of R peaks in the ECG signal to derive average HEPs from the continuous EEG recordings in the baseline condition.

In the wakefulness session (*Figure 3a,b*), we expected to observe omission HEP differences when comparing the synch to asynch and the synch to baseline conditions, as a consequence of the predictability of sound onset in the synch condition, based on the fixed delay between R peaks and sounds (see Pfeiffer and De Lucia, 2017 for similar findings). No such difference should be observed when comparing the asynch to baseline conditions. For the synch versus asynch comparison (*Figure 3b*), the cluster-based permutation test revealed a significant positive cluster ($p<0.05$) at 223 ms to 274 ms following R peak on posterior-central scalp electrodes. A significant negative cluster ($p<0.05$) at 162 ms to 267 ms following R peak was additionally observed in this comparison with two distinct peaks; an earlier peak at 162 ms to 213 ms located on anterior-central electrodes and a later peak at 217 ms to 267 ms located on posterior-lateral rightmost electrodes. The synch versus baseline comparison (*Figure 3a*) yielded one significant negative cluster ($p<0.005$) on posterior-central scalp electrodes at 36 ms to 275 ms. As anticipated, the asynch versus baseline comparison showed no significant differences.

In N2 sleep, we found differences between the omission HEPs of the synch and asynch conditions (*Figure 3c*) at -99 ms to 117 ms and at 322 ms to 500 ms following the R peak; both clusters were located on central electrodes. Similar to wakefulness, no significant clusters were identified for the asynch versus baseline comparison in N2 sleep. However, contrary to wakefulness results, contrasting the synch and baseline omission HEPs in N2 sleep revealed no significant differences between the two conditions. The same statistical tests carried out in the remaining sleep stages provided no significant results.

3.3. Sound-based omission response

In order to test our hypothesis that auditory regularities induced an expectation of incoming stimuli, we derived omission responses during sound omissions in the isoch and asynch conditions in wakefulness and all sleep stages (the analysis of the sound omission response in the synch conditions has been already

considered above in section 3.2). Average sound-based omission evoked potentials (OEPs) were calculated by extracting epochs from the continuous EEG recordings that were time-locked to the average sound interstimulus interval. A random selection of epochs were extracted from continuous baseline recordings, such that the latencies between epoch onset and closest heartbeat (i.e. R peak) were matched to the trial onsets in the sound-based isoch and asynch conditions at the single-trial level.

Based on previous reports of OEPs within regular auditory sequences during wakefulness *(e.g.* Chennu et al., 2016; van Laarhoven et al., 2017; SanMiguel et al., 2013a), here, we expected central negativity in the isoch condition (where temporal regularity existed in sound stimuli) between 100 ms and 250 ms, when compared to the asynch or the baseline conditions. Consistent with previous reports in the wakefulness session, the cluster-based permutation test comparing the isoch versus asynch condition yielded a significant negative cluster ($p<0.05$) at 226 ms to 288 ms following omission onset in central scalp electrodes (*Figure 3e*). The isoch versus baseline comparison (*Figure 3d*) revealed a significant negative cluster ($p<0.05$) at 103 ms to 170 ms following expected sound onset on anterior-central scalp electrodes. A second significant negative cluster ($p<0.05$) was observed for the same comparison at 251 ms to 295 ms following expected sound onset on posterior electrodes and a significant positive cluster ($p<0.05$) at roughly the same latency between 246 ms and 303 ms on anterior-central electrodes. Unexpectedly, the asynch versus baseline comparison in wakefulness also revealed a significant positive cluster ($p<0.05$) on central scalp electrodes at 197 ms to 288 ms following expected sound onset (*Suppl. Figure 2*).

Like omission HEPs, sleep OEP differences across auditory conditions were only significant in N2 sleep comparisons (*Figure 3f*). In addition, in accordance with omission HEP results, the isoch versus baseline and the asynch versus baseline comparisons during N2 sleep did not reveal significant differences. However, contrary to omission HEP findings, isoch versus asynch OEP differences were largely similar between wakefulness and N2 sleep, at least in terms of latency relative to expected sound onset. In more detail, statistical evaluation of the isoch and asynch condition differences (*Figure 3f*) identified a significant negative cluster ($p<0.05$) at 83 ms to 226 ms following expected sound onset localized to posterior-central scalp electrodes.

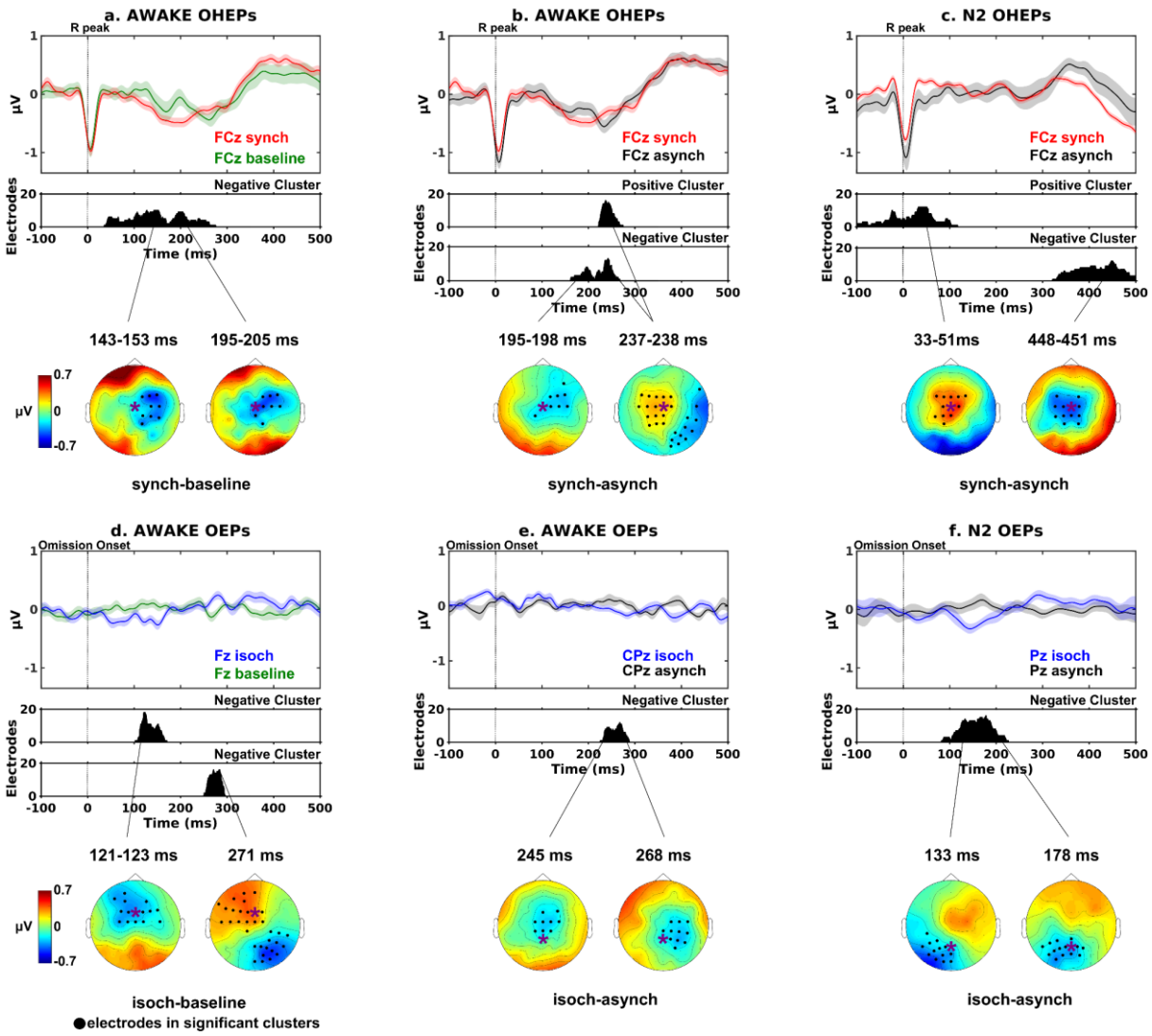

Figure 3. Neural omission responses in wakefulness and N2 sleep. Omission HEPs (OHEPs; time-locked to the R peak) and OEPs (time-locked to mean SS interval – expected sound onset) comparisons during sound omissions for the synch (red lines), asynch (black lines), isoch (blue lines) and baseline (green lines) conditions during wakefulness (AWAKE) and N2 sleep (N2). Significant differences are observed between the synch and baseline HEPs in wakefulness (a) and between synch and asynch HEPs in wakefulness (b) and N2 sleep (c), suggesting that the cardio-audio regularity induces a modulation of the HEP both in wakefulness and N2 sleep. In addition, the isoch regularity, *i.e.* with fixed sound-to-sound interval, induced significant differences between the isoch and baseline condition OEPs in wakefulness (d) and between the isoch and asynch condition OEPs in wakefulness (e) and N2 sleep (f). The OEP results suggest that fixed sound-to-sound regularity induced an expectation of incoming sounds, both during wakefulness and sleep. Top panels show grand average EEG waveforms for centrally-located representative electrodes in significant clusters, marked with a purple asterisk in the topographic representation. Middle panels display the number of electrodes within each significant cluster derived from cluster permutation statistical analysis ($p<0.05$, two-tailed). Bottom panels demonstrate topography differences at significant cluster peaks with significant electrodes highlighted in black.

4. Slow Oscillations Analysis

As outlined above (*Figure 3c*), the analysis of omission HEPs during N2 sleep (N=23) revealed that cardio-audio synchronization (compared to the asynch) gave rise to a central early onset positivity (at -99 ms to 117 ms) and late onset negativity (322 ms to 500 ms). This effect is reminiscent of the up and down states of slow oscillations (SOs) during N2 sleep (0.5-1.2 Hz oscillations; Massimini et al., 2004; Ngo et al., 2013; Nir et al., 2011). Indeed, the same analysis performed on 0.5 Hz to 4 Hz band-pass filtered EEG data (delta band; reflecting the range of SO frequencies) produced a highly similar profile for the synch against asynch omission HEPs during N2 sleep (results not shown). Specifically, in the delta frequency range comparison, an early onset central positivity difference ($p<0.05$) between -99 ms and 125 ms and a late onset central negativity difference ($p<0.05$) between 259 ms to 500 ms following heartbeat onset was identified.

In light of this observation and since sound presentations are known to alter the background oscillatory activity in sleep, notably the SOs during NREM sleep (Ngo et al., 2013; Ong et al., 2018; Schneider et al., 2020), we investigated whether the three auditory conditions had differential effects on the ongoing oscillations during N2 sleep. We selected the SO positive half-wave peak latency at electrode Cz as the representative SO latency and computed the median sound-to-SO latency for all auditory conditions and median R peak-to-SO latency for all auditory conditions and the baseline.

Statistical assessment using 1x3 repeated measures ANOVAs on the median sound-to-SO latencies yielded significant differences across auditory conditions (*Figure 4a*; $F_{(1,3)}=4.0$, $p<0.05$). Post-hoc pairwise comparisons confirmed much lower latencies in synch compared to asynch and in isoch compared to asynch ($p<0.05$). These results suggested a possible readjustment of the SOs with respect to sound onset depending on the regularity types (*Figure 4a*). When regularity is present, either in the synch or isoch conditions, SOs tended to align to the sound onset. Because of the fixed RS delay in the synch condition, the alignment between sound onset and SOs is also reflected in a lower heartbeat to SO peak in the synch compared to the asynch and isoch conditions (*Figure 4b*). In order to rule out that this SO readjustment was due to a specific relation between R peak and SO irrespective of sound presentation, we carried out a 1x4 repeated measures ANOVAs on the median R peak-to-SO latencies revealed significant differences across conditions (*Figure 4b*; $F_{(1,4)}=3.0$, $p<0.05$). These observed differences in median R peak-to-SO latencies were specific to the synch condition, as confirmed by the significantly lower median latencies ($p<0.05$) observed in synch compared to asynch and in synch compared to baseline.

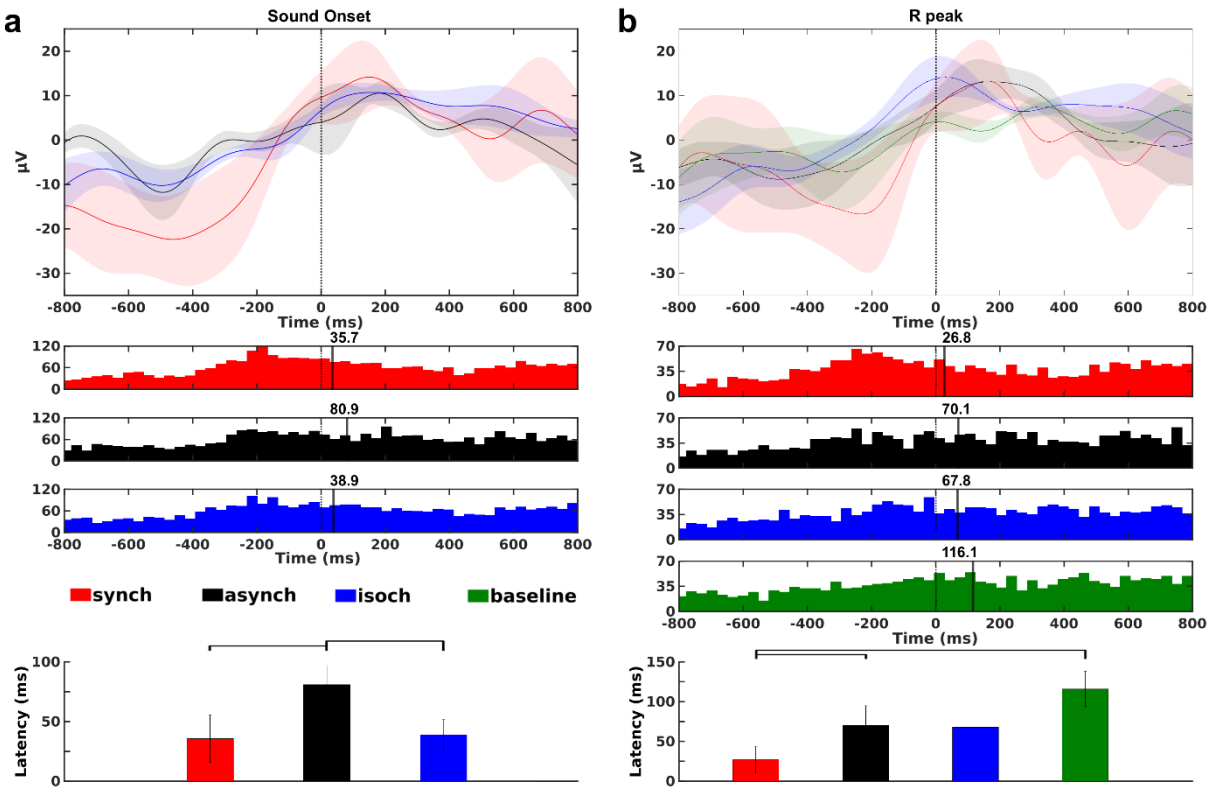

Figure 4. Modulation of SO activity by auditory stimulation in N2 sleep. Grand averaged SO waveforms at electrode Cz centered around sound onset (a) and R peak (b) in the synch (red lines), asynch (black lines), isoch (blue lines), and baseline (green lines) experimental conditions during N2 sleep (top panels). Histograms of the sound minus SO peak (a) and of the R peak minus SO peak (b) at electrode Cz across trials and participants for each condition (middle panels). Black vertical lines and associated text in the histograms depict the grand averaged median sound minus SO (a) and heartbeat minus SO (b) latency values. Grand averaged sound-to-SO latencies (a) and R peak-to-SO latencies (b) with statistically significant differences ($p<0.05$; black horizontal lines) across conditions (bottom panels). SO peaks are more likely to occur closer to the sound onset in the synch and isoch conditions than in the asynch conditions (a). These results are not trivially driven by a temporal proximity between R peaks and SO peaks in the synch condition as this is not observed during baseline (b).

5. Cardiac Omission Response

We further investigated whether omission responses could be observed across vigilance states in the RR intervals based on the ECG. To assess potential differences in temporal predictions across wakefulness and sleep stages, we analyzed heartbeat changes in response to sound omissions as a function of auditory conditions (synch, asynch, isoch).

5.1. Auditory condition contrast

We compared average RR intervals before, during and after omissions using two-way repeated measures ANOVAs with factors Auditory Condition (synch, asynch, isoch) and Trial Order (one trial before, trial during, first trial after, second trial after sound omissions) in wakefulness and sleep. To take full advantage of the available data in each vigilance state (*Suppl. Table 1 & 2*) separate repeated measures

ANOVAs were performed for each vigilance state (AWAKE, N1, N2, N3, REM where AWAKE refers to the separate wakefulness session). These analyses were conducted on normalized RR intervals (*Figure 5a,b*; by subject-wise division of each of the investigated average RR intervals by the average RR interval prior to sound omission), so that the results would not be attributable to inter-subject variability in RR interval values. Of note, analyses on non-normalized RR intervals displayed similar results (*Suppl. Figure 3).*

Overall, in wakefulness and sleep, we observed that cardio-audio synchronization led to an increase in the average RR interval during sound omissions (RR_{om}) compared to the trial before omission (RR_{-1}) that persisted over the following trial (RR_{+1}) and decreased over the second trial following omission (RR_{+2}). This deceleration in the heart rate upon sound omission was absent or inconsistent in the asynch and isoch conditions. Statistical analysis confirmed this difference across auditory conditions as follows.

3x4 repeated measures ANOVAs (AWAKE: N=26; N1: N=18; N2: N=24; N3: N=18; REM: N=17) revealed a significant interaction of Auditory Condition x Trial Order (see above) for all vigilance states (*Figure 5a*; AWAKE: $F_{(3,4)}=14.1$, $p<0.0005$; N1: $F_{(3,4)}=10.7$, $p<0.0005$; N2: $F_{(3,4)}=11.7$, $p<0.0005$; N3: $F_{(3,4)}=6.2$, $p<0.0005$; REM: $F_{(3,4)}=8.5$, $p<0.0005$) with a main effect of Trial Order (AWAKE: $F_{(1,4)}=20.1$, $p<0.0005$; N1: $F_{(1,4)}=6.7$, $p<0.005$; N2: $F_{(1,4)}=20.0$, $p<0.0005$; N3: $F_{(1,4)}=3.4$, $p<0.05$; REM: $F_{(1,4)}=7.7$, $p<0.0005$), and a main effect of Auditory Condition (AWAKE: $F_{(3,1)}=27.2$, $p<0.0005$; N1: $F_{(3,1)}=20.9$, $p<0.0005$; N2: $F_{(3,1)}=13.7$, $p<0.0005$; N3: $F_{(3,1)}=8.9$, $p<0.005$; REM: $F_{(3,1)}=24.1$, $p<0.0005$). Post-hoc pairwise t-tests corroborated that in the synch condition (*Figure 5a, red line*), omissions elicited a long-lasting heart rate deceleration, with higher RR interval during and immediately after the omission than before the omission across all vigilance states (AWAKE: $p<0.0005$; N1: $p<0.005$; N2: $p<0.0005$; N3: $p<0.05$; REM: $p<0.005$).

3.2. Vigilance State Contrast

To better characterize how sound omissions modulated RR intervals as a function of auditory conditions and vigilance states (*Figure 5b*), we computed a three-way repeated measures ANOVA with factors Vigilance State (AWAKE, N1, N2, N3, REM where AWAKE refers to the wakefulness session), Auditory Condition (synch, asynch, isoch), and Trial Order (one trial before, trial during, first trial after, second trial after sound omission), including all participants who had sufficient available data across all vigilance states (N=10; *Suppl. Table 2*).

The ANOVA revealed a significant main effect of Auditory Condition ($F_{(1,3,1)}=28.6$, $p<0.0005$), due to overall higher RR interval values (*i.e.* enhanced deceleration) during the synch condition, and a main effect of Vigilance State ($F_{(5,1,1)}=4.7$, $p<0.005$). Critically, replicating the analyses on separate vigilance states (*Figure 5a*), the interaction effect of Auditory Condition and Trial Order was also significant ($F_{(1,3,4)}=4.5$, $p<0.0005$). The interactions Vigilance State x Auditory Regularity ($F_{(5,3,1)}=1.0$, $p>0.05$), Vigilance State x Trial Order ($F_{(5,1,4)}=0.8$, $p>0.05$), and the triple interaction across all factors (Vigilance

State x Auditory Regularity x Trial Order; $F_{(5,3,4)}=0.5$, $p>0.05$) were not significant. This pattern of results further confirmed that the observed heart rate deceleration upon sound omission in the synch condition and lack thereof in the asynch and isoch conditions was consistent across vigilance states.

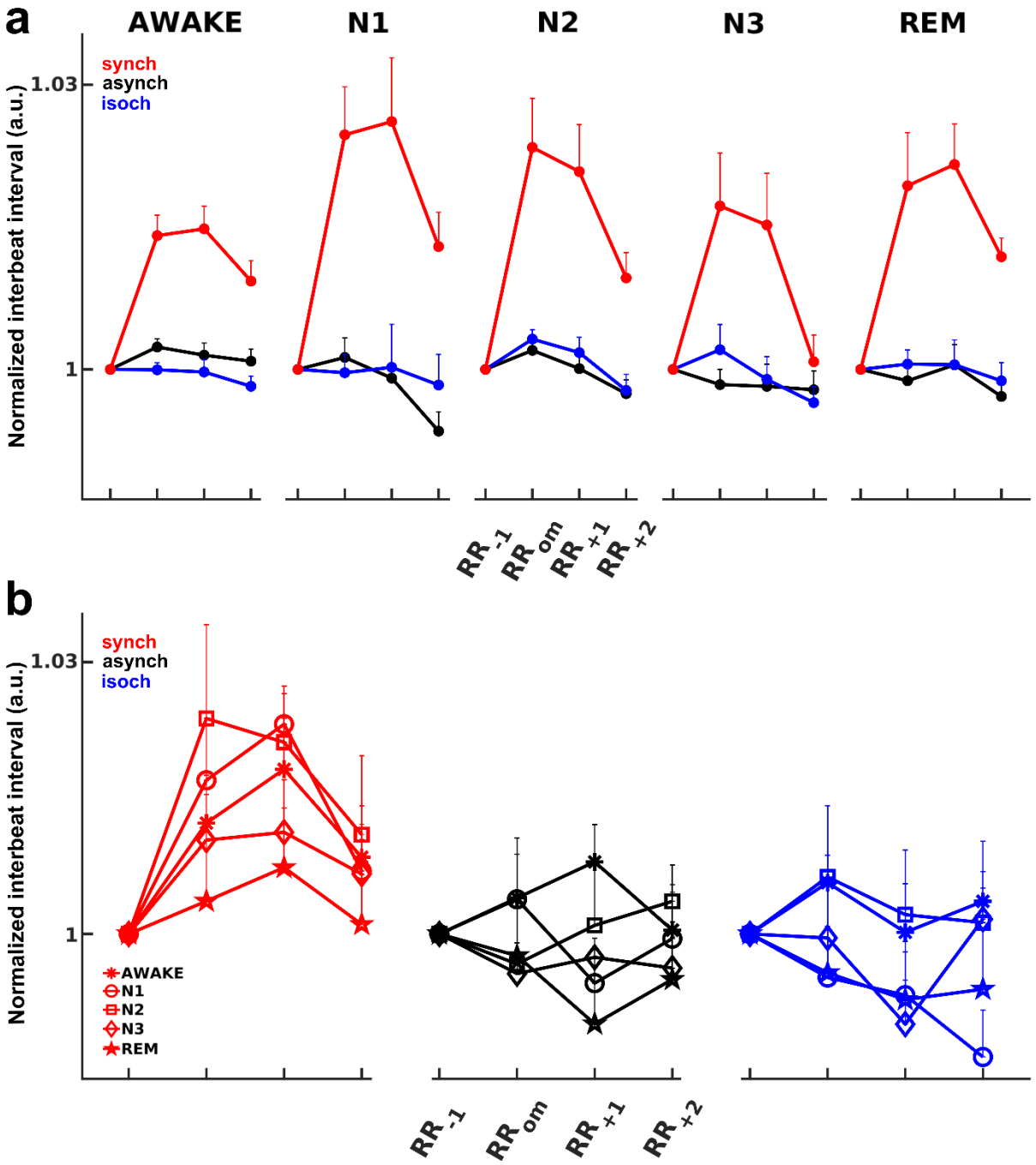

Figure 5. Cardiac omission response across auditory regularities in wakefulness and sleep. (a) Grand averaged normalized RR intervals prior (RR_{-1}), during (RR_{om}), and following (RR_{+1} and RR_{+2}) sound omissions across auditory conditions (synch: red line; asynch: black line; isoch: blue line) in the wakefulness session (AWAKE) and all sleep stages (N1, N2, N3, REM). (b) Grand averaged normalized RR intervals for participants with sufficient data across all vigilance states (N=10), prior (RR_{-1}), during (RR_{om}), and following (RR_{+1} and RR_{+2}) sound omissions in the wakefulness session (AWAKE, asterisks) and all sleep stages (N1, circles; N2, squares;

N3, diamonds; REM, pentagrams) for each auditory condition. Error bars indicate the SEM (upper limit). Overall, statistical analyses highlighted a heart rate deceleration upon sound omission in the synch condition across all vigilance states.

Discussion

We investigated the neural and cardiac correlates of cardio-audio regularity processing by administering sounds in synchrony to the ongoing heartbeat (synch), at fixed temporal pace (isoch), and in a control condition without specific temporal regularity (asynch) yet with similar sound-to-sound intervals across conditions in wakefulness and sleep. We hypothesized that auditory regularity encoding would result in a violation detection response as measured by the cardiac and neural signals upon unexpected omitted sounds. Neural responses to sound omissions revealed that sound sequences induced prediction of upcoming sounds both when temporally synchronized to the ongoing heartbeat and when sounds occurred at a fixed pace during wakefulness and N2 sleep. Enhanced prediction related to cardio-audio synchronization was also evident across all vigilance states in the form of a strong cardiac deceleration after sound omission. Analysis of the SOs background activity during N2 sleep revealed a reorganization of the ongoing brain activity both when sounds occurred in synchrony with the ongoing heartbeat and at fixed temporal pace. Taken together, our results highlight different mechanisms underlying the implicit ability of the human brain to make predictions about upcoming sensory stimuli during wakefulness and sleep.

Cardio-audio and auditory temporal regularity drives neural expectation in wakefulness

During wakefulness, the temporal coupling between cardiac and auditory inputs in the synch condition resulted in a different omission HEP (time-locked to the R peak) compared to the asynch condition and compared to the baseline condition (*Figure 3*). The observed positive peak at centrally located electrodes in the synch to asynch comparison around 240 ms (*Figure 3b*) closely matches previous results using a similar paradigm, where a difference of the same polarity and localization was observed at 260 ms (Pfeiffer and De Lucia, 2017). When considering the offset of 52 ms (*i.e.* average heartbeat to sound onset latency in the present study), the latencies of observed differences in the present study (synch versus asynch: 200 ms; synch versus baseline: 240 ms) fit well with previously reported classic omission responses between 150 ms and 200 ms (SanMiguel, Widmann, et al., 2013; van Laarhoven et al., 2017; Wacongne et al., 2011 and others). Moreover, during the synch condition, the cardio-audio synchronicity was essential for inducing the omission HEP response, as demonstrated by the lack of a differential omission HEP response between the asynch and baseline conditions when time locking to the R peak of the ECG signal.

Responses to classic sound omissions, exemplified by the OEPs, were observed in the same participants in the isoch condition (*i.e.* between 226 ms and 288 ms in the isoch against asynch, *Figure 3e*, and over 103 ms to 170 ms and 251 ms to 295 ms in the isoch against baseline comparisons, *Figure 3d*). The

timing of these differential responses extended to late onset latencies in comparison to classic omission responses in the literature, observed at 150 ms to 200 ms post-stimulus onset (SanMiguel, Widmann, et al., 2013; van Laarhoven et al., 2017; Wacongne et al., 2011 and others). A possible factor preventing a straightforward comparison to classic omission responses in previous studies was the individual adjustment of the sound-to-sound intervals, in order to match the average heartbeat. This resulted in a variable SS interval across participants and might have affected the violation detection signal (Schroger and Winkler, 1995). Another marked difference lies in the actual definition of omission responses. In our study, we looked at the difference between unexpected omissions in the isoch condition inducing both auditory and temporal prediction ('what' and 'when') against the asynch condition which can only generate an auditory prediction ('what' without 'when') (SanMiguel et al., 2013b). In previous reports, the omission response was instead derived by comparing conditions with different level of expectancy, as for example comparing expected versus unexpected sound omissions, revealing a violation detection response typically in the range of 100 ms and up to 200 ms post-stimulus onset (SanMiguel et al., 2013a; Wacongne et al., 2012). It is likely that in our analysis, the earliest of these effects was canceled as a result of having similar 'what' prediction about incoming sounds in both isoch and asynch. In addition, the early difference (~100ms) of central negative polarity in the isoch against baseline comparison can reflect the sensory template formation at the predicted sound onset occurring in the same period as the auditory N100 response (Dercksen et al., 2020; van Laarhoven et al., 2017, 2020; SanMiguel et al., 2013a; Wacongne et al., 2011).

Cardio-audio and auditory temporal regularity modulates neural omission responses in N2 sleep

During sleep, we showed both cardio-audio and auditory temporal regularity modulation of the omission responses in N2 sleep. First of all, OEPs during the isoch compared to the asynch conditions revealed a negative negative polarity difference at approximately 100 ms to 200 ms (Figure 3f). Since, to the best of our knowledge, no other studies in sleep have utilized omissions to study violation detection, we can only refer to the deviant sound literature in interpreting these results. Accordingly, the observed isoch versus asynch negative polarity is in line with the finding of the classic MMN response in NREM sleep (Sabri et al., 2002, 2003; Winter et al., 1995) and suggests an implicit tracking of the temporal relationship between sounds despite altered vigilance in N2 sleep. During the synch (compared to the asynch) condition, we found a positive cluster between -99 ms and 117 ms and a negative cluster between 322 ms and 500 ms (Figure 3c). The early central positivity observed in the synch against asynch omission HEPs could reflect auditory anticipation, while the later component could arise from a shifted MMN response, such a time shift in deviant stimulus typical electrophysiological signatures having been previously reported for the P300 response in N2 (Bastuji et al., 1995) and REM sleep (Sallinen et al., 1996).

Sound administration modulates SO activity in N2 sleep

The modulation of the omission HEP in N2 sleep prompted us to look into the possible influence of auditory stimulation on the background oscillatory activity. Indeed, the latencies and topography unveiled in the synch versus asynch N2 comparison (*i.e.* fronto-central positivity at -99 ms to 117 ms and fronto-central negativity at 322 ms to 500 ms) could reflect the up and down states of SOs during N2 sleep; keeping in mind that SO peak to trough latencies typically range between 400 ms to 1000 ms (reflecting 0.5-1.2 Hz oscillations; Massimini et al., 2004; Ngo et al., 2013; Nir et al., 2011). Here, this influence was demonstrated by a significantly reduced median latency between the sound stimulus onset and the peak of SOs (*Figure 4a*) for the synch (35.7 ms) and isoch (38.9 ms) conditions compared to the asynch (80.9 ms) condition. This indicates that sound presentations induced a modulation of slow oscillatory activity in N2 sleep in our subjects in such a way that, when temporal auditory predictions were high (*i.e.* synch and isoch), sound onset was more likely to occur close to the SO peaks. This evidence is reminiscent of the closed-loop auditory stimulation literature wherein temporary synchronization of sound stimuli to ongoing SOs induced an enhancement of the SO rhythm during NREM sleep (Besedovsky et al., 2017; Ngo et al., 2013; Ong et al., 2018; Schneider et al., 2020). In the present paradigm as well as in closed-loop auditory stimulation studies, the temporal proximity between sound onset and the SO positive peak suggests the existence of a preferential time window of stimulus processing which may coincide with the positive phase of the SO cycle when neuronal firing is maximal (Navarrete et al., 2020; Nir et al., 2011). On this basis, auditory regularities would induce a reorganization of the ongoing SO activity following encoding of auditory regularities, in order to facilitate the neural processing of expected sounds in a sequence when sound onset can be predicted (see also Zust et al., 2019 for consistent findings in associative learning bound to the SO peaks).

Of note, not only sounds have been shown to have an impact on the latency of SOs in NREM sleep. Lechinger and colleagues (2015) previously showed that R peaks tended to occur close to the positive peak of the SO compared to other latencies (Lechinger et al., 2015). With this in mind, we additionally investigated the potential impact of heartbeat signals on SOs (*Figure 4b*). In this study, we revealed significantly lower latencies between R peak onset and SO peak in the synch (26.8 ms) compared to the asynch (70.1 ms) and to the baseline (116.1 ms) conditions. This finding suggests that SO latency modulation by the ongoing heartbeat signal was specific to sound presentations temporally linked to heartbeats (*i.e.* in the synch) and is corroborated by the fact that we observed the highest heartbeat to SO latencies in the baseline condition where sounds were absent altogether.

Cardio-audio temporal regularity results in heart rate deceleration upon sound omissions

In addition to studying whether and how the brain might track regularities across cardiac and auditory inputs, we investigated the ECG responses to sound omissions as another potential marker of predictive coding. We found a deceleration of the heart rate during omissions across wakefulness and all sleep

stages that was most evident and consistently observed in the synch condition (*Figure 5*). One possible interpretation of the cardiac deceleration upon omission across vigilance states is in terms of attention reorientation following an unexpected and potentially dangerous event, a parasympathetically-driven effect often reported in conditioning paradigms (Pappens et al., 2014; Seligowski et al., 2021; Szeska et al., 2021). This response can also be associated to a startle reaction and a physiological freezing response, linked to heart rate deceleration, pupil dilation and skin conductance alterations (Blanchard et al., 2011; Gladwin et al., 2016; Jennings and Van Der Molen, 2005; Lojowska et al., 2015; Roelofs, 2017). The heart rate deceleration upon threat detection may result from cholinergic system engagement, which modulates arousal, with similar mechanisms observed in rats when awakened from NREM sleep by activation of basal forebrain cholinergic neurons using chemical and optogenetic techniques (McKenna et al., 2020; Zant et al., 2016). Yet, another plausible explanation for the heart rate deceleration following unexpected omission in the synch condition relates to top-down adjustment of cardiac rhythm in order to account for the unexpected silence. As a sound is predicted following a heartbeat (in the synch condition), the omission may prolong the generation of the next heartbeat within physiologically plausible boundaries so as to 'wait' for a delayed auditory stimulus within the sequence, followed by a rapid readjustment to the original rhythm upon subsequent sound presentations. By construction, unlike the synch condition where the heartbeat deceleration was consistently observed, such deceleration was either highly reduced or absent in conditions where sound presentations bear no temporal relation to ongoing heartbeats (*i.e.* asynch and isoch conditions).

In summary, both threat detection and the interplay between interoceptive and exteroceptive stimulus processing provide plausible interpretations for the cardiac response to sound omission in different regularity types, and complement previous findings on the alternative neural mechanisms underlying sensory encoding in sleep (Andrillon et al., 2017; Hennevin et al., 2007; Kouider et al., 2014; Nir et al., 2015; Sela et al., 2016).

Limitations

First, participant selection involved an informal interview assessing each individual's sleep quality, without a systematic sleep quality evaluation based on questionnaires or actigraphy monitoring, as is common practice in sleep research (Ibáñez et al., 2018). This, along with the absence of an adaptation night of sleep for participants to familiarize themselves with the sleep laboratory conditions, could have resulted in a participant cohort with heterogeneous sleep characteristics. Nonetheless, considering the type of stimulation performed in this study, polysomnographic sleep assessment during the experimental nights demonstrated sufficient sleep quality and comparable results to the literature (*e.g.* Perogamvros et al., 2019).

Second, the comparison between wakefulness and sleep results is limited by the differences in the experimental design between the two sessions. Indeed, during sleep, baseline administration was

intermixed with auditory stimulation, while in the wakefulness data acquisition, the baseline was administered only once at the start of the experiment when participants were still familiarizing themselves with their new environment. While this was chosen to prevent fatigue due to long acquisition times in the wakefulness session and to ensure a representative baseline across sleep stages in the sleep session, this could have caused elevated heart rate and reduced heart rate variability in wakefulness, until participants finally settled with the experimental setting (*Suppl. Figure 1g,h*).

A third limitation of the present study is the low number of participants providing sufficient EEG based artifact-free trials in N1, N3 and REM sleep (*Suppl. Tables 1 & 2 & 3*). It therefore remains unresolved whether the lack of neural omission responses during these sleep stages resulted from a low statistical power or was due to truly impaired auditory regularity processing and deviance detection. The analysis of the cardiac response to unexpected omissions suggests that auditory regularity processing, especially when induced by the cardio-audio coupling, is preserved across all sleep stages and would possibly be detectable at the neural level provided sufficient available data. What also emerges from this limitation is a possible strength of the cardiac omission response. Detecting the heart rate deceleration with a measure as easily obtained and artifact-free as the ECG signal could offer a simple and reproducible biomarker of the preservation of sensory regularity processing in health and disease. In line with this proposal, recent work posits that the analysis of heart rate fluctuations may be informative of the degree of preservation of conscious sensory processing in healthy populations and disorders of consciousness patients (Endoh et al., 2019; Pérez et al., 2021; Raimondo et al., 2017; Riganello et al., 2022). A further investigation into the origin of the cardiac omission response through the measure of pupil dilation, respiration or changes in skin conductance will help identify to what extent this response is a consequence of the autonomic nervous system activity.

In addition, as the heartbeat evoked responses during sound omission are contaminated by the heartbeat related artifacts, differential neural responses to sound omission across conditions could be trivially due to differences between these artifacts. In our study, we could reasonably exclude this confounding factor when interpreting the differences in the heartbeat evoked responses because of the highly similar ECG signal waveforms during the omission period across auditory conditions and both in wakefulness and sleep. The only difference was observed when comparing the baseline average ECG waveforms to that of the synch and the asynch conditions which nevertheless occurred at different latencies that those emerging from the comparison of the omission HEPs.

A final possible confound to mention relates to how sensory processing is influenced by the stimulus onset relative to the cardiac cycle (Adelhöfer et al., 2020; Kimura, 2019; Kunzendorf et al., 2019; Petzschner et al., 2019; Pfeifer et al., 2017; Waselius et al., 2018), thought to rely on whether stimulus presentation occurs within the systole or diastole period (Adelhöfer et al., 2020; Al et al., 2020). Although in our case, the latencies of sound onset and periods of investigation are solely within the

systole range, the slower heart rate in sleep in comparison to wakefulness may have resulted in sounds being presented at different timings within the cardiac cycle across vigilance states. Nonetheless, within the range of the systole period, we expect that sensory processing would be similar within this range (Al et al., 2020) and in both wakefulness and sleep. In support of this, we already verified that changes of the order of 10 ms between R peak and sound onset produce similar results in the comparison between synch and asynch in wakefulness, upon consideration of the different average RS interval in the synch condition for this study, M = 52 ms, and an earlier study with M = 41 ms (Pfeiffer and De Lucia, 2017).

Key Contributions

The experimental paradigm implemented herein has several advantages over previous investigations into the role of heartbeat signals in auditory regularity processing. First, the use of omissions as opposed to deviant sounds commonly employed in sleep MMN investigations (*e.g.* Ruby et al., 2008; Sculthorpe et al., 2009; Strauss et al., 2015) and interoceptive-auditory stimulus interactions (Van Elk et al., 2014) allows for a direct investigation of sensory regularity encoding, free from bottom-up auditory stimulus contributions. Second, this experimental paradigm enabled a counterbalanced ECG artifact between the synch, asynch and baseline conditions when contrasting the omission HEPs time-locked to the R peaks. Third, by investigating both wakefulness and sleep in the same healthy volunteers, we now demonstrate that the human brain infers on the temporal relationship across cardiac and auditory inputs in making predictions about upcoming auditory events across vigilance states. Finally, in the current investigation, we did not only focus on potential neural responses to omissions but additionally identified a cardiac decelaration as a result of violation detection. Importantly, this cardio-audio synchronicity created *ad hoc* in the experimental environment might reflect real life readjustment of the heartbeat rhythm in order to optimize the temporal relationship between bodily signals and exteroceptive inputs for optimal sensory encoding.

Conclusion

Collectively, the present results suggest that the human brain can keep track of temporal regularities between exteroceptive inputs, and across interoceptive and exteroceptive inputs during both wakefulness and sleep. Inferring on this relationship may allow humans to form predictions about upcoming sensory events and may aid violation detection when such predictions are unfulfilled. Our findings replicate earlier findings in wakefulness (Pfeiffer and De Lucia, 2017) and support theories for an interoceptive predictive coding mechanism (Park and Blanke, 2019; Park and Tallon-Baudry, 2014; Seth et al., 2012). To our knowledge, this is the first study to investigate auditory regularity processing using omissions and to offer evidence for a potential role of interoceptive inputs under the predictive coding framework in sleep. The conscious and unconscious brain may implicitly process relationships across interoceptive and exteroceptive inputs in order to optimize the signaling and prediction of potential upcoming dangers.

Methods

Ethics Statement

Approval for the study was obtained by the local ethics committee (La Commission Cantonale d'Ethique de la Recherche sur l'Etre Humain), in accordance with the Helsinki declaration.

Study Population

Twenty-six self-reported good sleeper volunteers took part in both the wakefulness and sleep arms of this study. Participants were considered eligible if they had no history of psychiatric, neurological, respiratory or cardiovascular conditions, no sleep apnoea, and a regular sleep schedule, evaluated during a phone interview. Hearing conditions were an additional exclusion criterion. All participants gave written informed consent and received roughly 150 Swiss Francs as monetary compensation.

Experimental Design

A two-way crossover experimental design was implemented in this study. Participants attended one wakefulness and one sleep session on two occasions separated by a minimum of one day and a maximum of ten days (wakefulness session first for 12 out of 26 participants). In both sessions, participants were instructed to passively listen to the administered sound sequences. They were naïve to the experimental manipulation, as suggested by informal verbal inquiry regarding the experimental design after the experiment. At the end of the second session, and if desired, participants were debriefed about the purpose and design of the experiment.

The sleep session recordings took place in a sound-attenuated hospital room equipped with a comfortable hospital bed to allow for overnight sleep recordings. During the sleep session, participants arrived at the laboratory at approximately 9 pm and following set-up preparation, they were instructed to lie down and inform the experimenters when they were ready to sleep. Lights were then switched off, the auditory stimulus administration commenced and the volunteers were left alone to naturally fall asleep. Although participants had the liberty to leave at any time, we explained that their inclusion in the study required a minimum of four hours of continuous data acquisition after sleep onset. They were free to choose to spend the night at the sleep laboratory and to be woken up at a desired time or by approximately 7 am the next morning, at which time lights were switched on.

In both sessions, participants were equipped with electrodes for heartbeat (ECG), eye movement (EOG), and EEG recordings (see below). For the sleep session, additional electrodes for submental electromyography (EMG) were attached, in accordance with the 2007 AASM guidelines for sleep scoring (Iber et al., 2007). In-ear phones (Shure SE 215, Niles, IL) were utilized during both sessions instead of external headphones, in order to increase sound attenuation, subject comfort during sleep and to prevent physical contact with and thus displacement of EEG cap and electrodes. The online EEG,

ECG, EOG and EMG were continuously monitored by the experimenters to ensure effective stimulus administration, data acquisition, heartbeat detection and sleep quality throughout both sessions.

Assessment of sleep onset was qualitatively inspected by monitoring the electrophysiological signals in real-time to identify well-known sleep markers in accordance with Iber et al. (2007). Specifically, indicative of sleep onset in the EEG signals, were the dissipation of low-amplitude alpha (8-13 Hz) posterior activity, the appearance of high-amplitude slow wave activity (1-4 Hz) and observable K complexes or sleep spindles. In addition, the reduction in eye movements and muscle tone demonstrated that volunteers were asleep, as observed in the EOG and submental EMG peripheral electrophysiological signals, respectively.

Stimuli

Sound stimuli were 1000 Hz sinusoidal tones of 110 ms duration (including 7 ms rise and fall times) and 0 μs inter-aural time difference. A 10-ms linear amplitude envelope was applied at stimulus onset and offset to avoid clicks. Stimuli were 16-bit stereo sounds sampled at 44.1 kHz and were presented binaurally with individually adjusted intensity to a comfortable level for wakefulness. A considerably lower than wakefulness intensity of approximately 45 dB was chosen for sleep, in order to facilitate a non-fragmented sleep session without multiple awakenings.

Experimental Procedure

During the wakefulness session, volunteers sat comfortably on a chair in a sound-attenuated experimental room and were instructed to keep their eyes open, avoid excessive eye blinking, body and jaw movements, and to breathe regularly; the aforementioned measures served in ensuring high signal quality. Each participant was presented with four types of stimulation conditions administered in separate experimental blocks in a pseudo-random order and was asked to passively listen to the sounds while keeping the eyes fixed on a cross centrally located in the visual field. The conditions were a baseline without auditory stimulation and three auditory conditions, namely synch, asynch and isoch. During wakefulness, the baseline lasted ten minutes and was acquired prior to auditory stimulation. During sleep, numerous two-minute baseline blocks were acquired in alternation to the sound sequences in an attempt to ensure that baseline background activity was comparable to the preceding sound stimulation during all stages of sleep. The three auditory conditions lasted five minutes each and corresponded to separate experimental blocks, which were repeated six times during wakefulness in a semi-randomized order. During the sleep session, the auditory condition five-minute blocks were administered for the entire length of the sleep recording in sequences of three auditory blocks always followed by a baseline (*e.g.* isoch-synch-asynch-baseline or synch-asynch-isoch-baseline). Randomization of the auditory condition order accounted for temporal effects (*i.e.* fatigue, habituation) on EEG recordings.

Auditory Conditions

All auditory conditions consisted of the sequential presentation of 250 stimuli (80% sounds and 20% omissions) administered in a pseudo-random order wherein at least one sound stimulus intervened between two subsequent omissions. In addition, in all auditory conditions, sound-to-sound intervals were sufficiently large in both the wakefulness and sleep session across all volunteers to ensure no overlap of subsequent sound stimuli with the main components of the AEP. Details for each auditory condition are given below and a thorough post-hoc evaluation of the experimental manipulation is provided in the Results and Supplementary Material (*Results 2. Quality Control Analyses & Suppl. Figure 1*).

In the synch condition, the temporal onset of each sound stimulus was triggered by the online detection of R peaks from raw ECG recordings. To enable effective online R peak detection, raw ECG recordings were analyzed in real-time using a custom MATLAB Simulink script (R2019b, The MathWorks, Natick, MA). The variance over the preceding 50 ms time window was computed and an R peak was detected when the online ECG value exceeded an individually adjusted 10–15 mV^2 variance threshold, which in turn triggered the presentation of a sound stimulus or an omission. This procedure resulted in a fixed R peak to sound average delay (*i.e.* RS interval) of 52 ms (SD = 5 ms) for wakefulness and 54 ms (SD = 7 ms) for sleep across participants.

In the asynch condition, the onset of sound presentation was based on the RR intervals extracted from a previously acquired synch block. Specifically, the ECG recorded during the preceding synch block was analyzed offline to extract RR intervals by automatic detection of R peaks and computation of RR intervals. 250 RR intervals were selected if they were above the 25th and below the 75th percentile of RR interval distribution in the synch block, in order to take into account possible missed R peaks in the online detection during the synch block. Next, RR interval order was shuffled giving rise to a predefined pseudo-random sequence closely resembling the participant's heartbeat rhythm. By construction, differences between the synch and asynch conditions in terms of average and variance of the RR intervals were minimized, contrary to the RS interval being fixed in the synch condition and variable in the asynch condition. The variable sound to heartbeat relationship resulted in an average RS interval of 4 ms (SD = 10 ms, range = −22 to 21 ms) for wakefulness and -3 ms (SD = 29 ms, range = -70 to 42 ms) for sleep, as well as an average SR interval of 742 ms (SD = 108 ms, range = 504-975 ms) for wakefulness and 882 ms (SD = 145 ms, range = 677-1188 ms) for sleep.

In the isoch condition, the onset of sound presentations was based on the median RR interval calculated during a previously acquired synch block. In more detail, the ECG recorded from the preceding synch block was analyzed to extract RR intervals via automatic detection of R peaks and computation of the median RR interval in set synch block, which served as the sound-to-sound interval for the construction of an isochronous auditory sequence. This procedure produced largely similar sound-to-sound intervals

across the synch, asynch and isoch conditions. Importantly, unlike the synch and asynch conditions, this procedure resulted in fixed sound-to-sound intervals with low variability (*i.e.* SS variability: SEM of SS interval) of 1.2 ms for wakefulness and 5.0 ms for sleep across participants. Similar to asynch, in the isoch condition, the variable sound to heartbeat relationship resulted in an average RS interval of 7 ms (SD = 21 ms, range = −36 to 57 ms) for wakefulness and -1 ms (SD = 29 ms, range = -58 to 56 ms) for sleep, in addition to an average SR interval of 743 ms (SD = 106 ms, range = 516-997 ms) for wakefulness and 893 ms (SD = 153 ms, range = 673-1210 ms) for sleep.

Data Acquisition

Continuous EEG (g.HIamp, g.tec medical engineering, Graz, Austria) was acquired at 1200 Hz from 63 active ring electrodes (g.LADYbird, g.tec medical engineering) arranged according to the international 10–10 system and referenced to the right ear lobe. Biophysical data were acquired using single-use Ag/AgCl electrodes. Three-lead ECG was recorded by attaching two electrodes (a third was a reference) to the participant's chest on the infraclavicular fossae and above the heart. A vertical EOG electrode was attached below the right eye and a horizontal EOG electrode was attached to the outer right canthus. Since changes in muscle tone are associated with alterations in consciousness during sleep and are an essential marker for effective sleep staging (Iber et al., 2007), EMG was additionally acquired sub-mentally during the sleep session alone. Impedances of all active electrodes were kept below 50 kΩ. All electrophysiological data were acquired with an online band-pass filter between 0.1 and 140 Hz and a band-stop filter between 48 and 52 Hz to reduce electrical line noise.

Sleep Scoring

An experienced sleep scoring specialist (Somnox SRL, Belgium), blind to the experimental manipulation in this study, performed the scoring of the continuous sleep electrophysiological data in order to pinpoint the periods of wakefulness and micro-arousal as well as periods of N1, N2, N3 and REM sleep. Sleep scoring was performed via visual inspection of contiguous 30-second segments of the EEG, EOG and EMG time-series, as outlined in the 2007 AASM guidelines for sleep scoring (Iber et al., 2007). Segments scored as periods of wakefulness or micro-arousals in the sleep recordings were excluded from further analysis.

Data Analysis

Electrophysiological data analyses were performed in MATLAB (R2019b, The MathWorks, Natick, MA) using open-source toolboxes EEGLAB (version 13.4.4b, (Delorme and Makeig, 2004)), Fieldtrip (version 20201205, (Oostenveld et al., 2011)), as well as using custom-made scripts.

R peak Detection

The R peaks in the continuous raw ECG signal were selected offline using a semi-automated approach as in Pfeiffer & De Lucia (2017). The custom-made MATLAB script, *rpeakdetect.m* (https://ch.mathworks.com/matlabcentral/fileexchange/72-peakdetect-m/content/peakdetect.m), was utilized to automatically identify the sharp R peaks in the raw ECG signal. Visual inspection of the online and offline detected R peaks ensured that the selected peaks fitted within the expected structure of the QRS complex in the continuous raw ECG signal. Frequent flawed online identification of the R peaks in a given block resulted in the exclusion of the block from a given participant's dataset. For blocks that were included, unrealistic RR, RS and SR interval values, observed as a result of infrequent flawed offline marking of R peaks, were identified and excluded using the *rmoutliers* MATLAB function (R2019b, The MathWorks, Natick, MA) and visual inspection of the detected R peaks and selected outliers.

Quality Control Analysis

A series of control analyses were performed to investigate possible overall differences in RR and SS intervals across conditions that might have confounded the present results. RR and SS intervals (for sound trials preceded by sound trials) were extracted for the synch, asynch, isoch and baseline conditions where relevant. In addition, RS intervals for sound trials and SR intervals for omission trials were computed to quantify the degree of cardio-audio synchronization and heartbeat onset variability during sound omission, respectively. Variability in the same interval measures, computed as the SEM was additionally investigated. Of note, unlike RR, SR and RS variability, SS variability was first computed within a given experimental block and then across experimental blocks, to account for ongoing changes in RR intervals (and hence SS intervals) in sleep. One way repeated measure ANOVAs ($p < 0.05$) were performed on the average RR, SS, RS and RS intervals and variabilities of each participant at wakefulness and all sleep stages with within-subject factor Condition (3 levels for SS, RS, SR intervals and variability: synch, asynch, isoch; 4 levels for RR intervals and variability: synch, asynch, isoch, baseline). Post-hoc t-tests ($p < 0.05$) identified any significant pairwise comparisons. To ensure no significant differences in the ECG signal across experimental conditions, ECG waveforms were extracted from ECG recordings between -100 ms and 500 ms relative to the R peak onset, matching the EEG trial-based analysis (see below, *EEG Data Analysis*). 1x4 repeated measures ANOVAs ($p<0.05$) with factor Auditory Condition (synch, asynch, isoch, baseline) were performed for each time-point in the average ECG waveforms and a False Discovery Rate procedure (Benjamini and Hochberg, 1995) was adopted to correct from multiple comparisons across time-points. Post-hoc t-tests ($p < 0.05$) allowed for the identification of significant differences between the compared conditions.

EEG Data Analysis

Continuous raw EEG data were band-pass filtered using second-order Butterworth filters between 0.1 and 40 Hz for the wakefulness session and 0.5 and 30 Hz for the sleep session. A larger high pass cut-off was chosen for sleep electrical signals in order to exclude periodic breathing and sweating artifacts which may occur in that frequency range in sleep and a lower low-pass cut-off was employed in agreement with the sleep literature (*e.g.* Ngo et al., 2013). To look specifically at slow oscillatory activity (*Results 4. Slow Oscillation Analysis*), raw electrophysiological data were band-pass filtered between 0.5 and 4 Hz, a well-established frequency range for investigations of slow-wave activity in the delta band range (Bouchard et al., 2021).

Ocular and muscular activity in the continuous EEG was identified for wakefulness data by performing Independent Component Analysis (ICA) as implemented in Fieldtrip (Delorme and Makeig, 2004; Oostenveld et al., 2011) and any selected eye movement or muscle activity related components were removed. We refrained from applying the ICA algorithm to the continuous sleep EEG data since changes in periodic eye movements and muscle activity form an integral part of the human sleep cycle. Therefore, contrary to wakefulness, excluding ocular and muscular contributions to the acquired EEG signal may have resulted in loss of relevant activity in sleep electrophysiology.

Wakefulness and sleep continuous EEG data were epoched between -100 ms and 500 ms relative to the selected event onset. This range was chosen in reflection of previously reported classic omission response latencies (SanMiguel, Widmann, et al., 2013; van Laarhoven et al., 2017; Wacongne et al., 2011 and others) and importantly, to ensure no overlap between consecutive auditory stimulation trials (as in Pfeiffer & De Lucia (2017), assuming a range of 60-100 beats per minute across volunteers). Various event onsets were selected, namely, heartbeat onset, sound onset and omission onset, depending on the comparison performed (*Results 3. Neural Omission Response*). Of note, while the isoch condition had fixed SS intervals (with an expected slight jitter due to the equipment), this was not the case in the asynch condition. To test whether sound prediction was based on computing the time of maximal sound occurrence probability, average sound-based omission responses were calculated by extracting epochs from the continuous EEG asynch and isoch recordings, now time-locked to the latency occurring during the omission at the average SS interval.

The resting-state baseline recordings acquired as part of the experimental procedure (without auditory stimulation) were utilized to extract EEG evoked potentials with matched event onsets to auditory stimulation trials and epoched between -100 ms and 500 ms. First, we extracted HEPs based on heartbeat onset in the resting state for upcoming statistical comparisons to the synch and asynch HEP. Second, in the absence of sound stimulation, the baseline allowed for comparing the OEPs of the isoch and asynch conditions to a control condition. In this case, a random selection of epochs was extracted from continuous baseline recordings, such that the latencies between epoch onset and closest heartbeat (*i.e.*

R peak) were matched on the single-trial level to the trial onsets in the sound-based isoch and asynch conditions. Upcoming pre-processing steps were replicated for auditory stimulation and baseline trials, for each participant, and for wakefulness and all sleep stages as follows.

Artifact electrodes and trials were identified using a semi-automated approach for artifact rejection as implemented in Fieldtrip (Oostenveld et al., 2011). Noisy EEG electrodes were excluded based on a signal variance criterion (3 z-score Hurst exponent) and substituted with data interpolated from nearby channels using spherical splines (Nolan et al., 2010). Across eligible participants, an average of 7.3 (SD: 2.2) electrodes (M: 11.7%, SD: 3.6%) were interpolated in wakefulness and an average of 8.9 (SD: 1.1) electrodes (M: 14.4% SD: 1.7%) were interpolated in sleep. Extended recording lengths, participant sweating, and head and body movement during the night could account for the greater number of artifactual electrodes observed in sleep recordings. In wakefulness data, trials containing physiological artifacts (*e.g.* eye movement, excessive muscle activity), not accounted for by ICA, were identified by visual inspection and by using a 70 μV absolute value cut-off applied to the EEG signal amplitude and were excluded from further analysis. A higher absolute value threshold of 300 μV was employed for the selection of artifactual epochs in sleep, in order to prevent the exclusion of high-amplitude slow wave activity (Andrillon et al., 2017). Extreme outliers in signal kurtosis and variance were additional criteria for the rejection of artifactual trials from sleep recordings.

The 30-second sleep stage labeled epochs were used to label artifact-free trials for all event onset types and for all three auditory conditions and the baseline. Hence, five different sets of trials formed the final processed dataset per participant for each of the five vigilance states: AWAKE, N1, N2, N3 and REM sleep where available (*Results 1.1. Participants & Suppl. Tables 1 & 2*). We note that we chose not to employ pre-stimulus baseline correction in wakefulness or sleep trials. In addition, since one way ANOVAs on artifact-free trials numbers for each evoked response of interest confirmed that no significant differences in trial numbers existed across auditory conditions alone, all trials were kept in auditory condition comparisons (*Suppl. Table 3*). Conversely, since acquired baseline data were significantly less than the three auditory conditions, in the case of group level comparisons to the baseline, trial numbers were quantitatively matched for each participant and for each vigilance state between auditory conditions and baselines. Finally, grand average evoked responses to sound omissions were derived.

EEG Statistical Analysis

EEG statistical analyses were performed in MATLAB (R2019b, The MathWorks, Natick, MA) using Fieldtrip (version 20201205, (Oostenveld et al., 2011)), as well as custom made scripts. For the analysis of the electrophysiological signals during the wakefulness and sleep sessions, we imposed a minimum of 60 artifact-free trials for the EEG data analysis, chosen based on the signal-to-noise ratio required to meaningfully interpret EEG statistical analysis results (Luck, 2005).

The non-parametric cluster-based permutation statistical analysis approach (Maris and Oostenveld, 2007) was employed to investigate sensor-level EEG-based differences between the various experimental conditions outlined herein. Under this statistical framework, statistically significant individual data samples were grouped based on the degree of their shared spatial and temporal characteristics. The resulting clusters were statistically evaluated by summating the t-values for all samples forming up a given cluster. In order to reject the null hypothesis that no significant differences existed in the given set of experimental conditions being contrasted, maximum cluster-level statistics were determined by shuffling condition labels (5000 permutations), allowing for a chance-based distribution of maximal cluster-level statistics to be estimated. Since maxima are utilized by this method, it enables the correction of multiple comparisons in time and space. A two-tailed Monte-Carlo p-value allowed for the definition of a threshold of significance from the distribution ($p < 0.05$, two-tailed). In wakefulness, this procedure was performed from 0 ms to 350 ms relative to the event onset of interest (heartbeat onset for omission HEP comparisons and average SS interval for OEP comparisons). The aforementioned time window was chosen in reflection of a previous publication from our laboratory (Pfeiffer and De Lucia, 2017), suggesting that changes of interest occurred within the selected period. Conversely, in sleep and in the absence of prior knowledge specific to this paradigm, we chose to apply cluster-based permutation statistics over the entire epoch length from -100 ms to 500 ms relative to event onset.

SO Data Analysis

To examine whether N2 sleep EEG statistical analysis results could have been influenced by the relationship between sounds and SO activity (Besedovsky et al., 2017; Ngo et al., 2013; Schneider et al., 2020) and/or between heartbeats and SO activity (Lechinger et al., 2015) in NREM sleep, we identified SOs in N2 sleep artifact-free EEG data and computed the latency at which they occurred compared first, to sound presentations in the auditory conditions and second, to heartbeats in the auditory conditions and baseline.

SO Detection

SOs in the continuous EEG time-series were detected across experimental conditions over frontocentral electrode Cz where a high probability for SO detection is to be expected (Massimini et al., 2004). We marked SOs based on the method described in Ngo et al. (2013) and more recently in Besedovsky et al. (2017). In brief, the 0.5 to 30 Hz band-pass filtered data were downsampled from 1200 Hz to 100 Hz and a low pass finite impulse response filter of 3.5 Hz was used in order to improve the detection of SO components. Next, N2 sleep labeled segments were extracted for the identification of SOs. Consecutive positive-to-negative zero crossings were picked out and were selected only if their temporal distance was between 0.833 s and 2 s, yielding a frequency between 0.5 Hz and 1.2 Hz for the designated oscillations. Negative and positive peak potentials in the oscillations were defined as the minima and

maxima present within eligible consecutive positive-to-negative zero crossings. The mean negative and mean positive to negative amplitude differences were calculated across selected oscillations at electrode Cz. For each identified oscillation that satisfied the frequency criterion, if the negative amplitude was 1.25 times lower than the mean negative amplitude and the positive to negative amplitude difference was 1.25 times higher than the mean positive to negative amplitude difference, the oscillation was marked as a SO.

Sound or Heartbeat to SO Latency Calculation

The positive half-wave peak time point was chosen as the representative latency for each SO in light of relevant literature (Navarrete et al., 2020; Nir et al., 2011) and following visual inspection of the SO and sound presentation time-series. Sound to SO latency for the synch, asynch and isoch conditions and R peak to SO latency for the synch, asynch, isoch and baseline conditions were computed for all artifact-free sound trials. Omission trials were excluded from this analysis since in this case, we were interested in how sounds and the sound to heartbeat relationship may modulate SOs in N2 sleep. Latencies were considered as valid only if they were between -800 and 800ms, a range chosen to minimize potential contamination of the sound or R peak to SO relationship by upcoming sounds or heartbeats. Median latencies were calculated for each subject and condition separately.

Sound or Heartbeat to SO Statistical Analysis

In N2 sleep, 1x3 repeated measures ANOVAs were calculated on the median sound to SO latencies at electrode Cz with within-subject factor Auditory Condition (synch, asynch, isoch) and 1x4 repeated measures ANOVAs were computed on the median heartbeat to SO latencies with within-subject factor Condition (synch, asynch, isoch, baseline). Pairwise comparisons were calculated using post-hoc t-tests between all investigated within-subject variables. Latency trial numbers were matched for the median heartbeat to SO latency comparison but not for the sound to SO latency comparison, since in the former, baseline recordings lengths were significantly lower to auditory condition recordings (as confirmed by 1x4 and 1x3 repeated measures ANOVAs on latency trial numbers, which significantly differed only across heartbeat to SO trials and not sound to SO trials).

ECG Data Analysis

The identified R peaks were used to derive omission trial related RR intervals. The representative R peak for an omission trial was selected as the first R peak following an omission in the continuous ECG signal. The omission RR Interval (RR_{om}) was therefore calculated as the latency between the selected omission R peak and the R peak immediately preceding it. In order to investigate potential heartbeat alterations associated with the omission trial, additional RR intervals were identified using contiguous R peaks to reflect the RR interval for the trial prior to omission (RR_{-1}) and up to two trials following

omission (RR_{+1} and RR_{+2}). Omission trials were considered only if they were followed by at least two sound stimuli to ensure no overlap between investigated RR intervals.

The 30-second sleep stage labeled epochs were used to label omission trials for all auditory conditions. For the analysis of the ECG signals during the wakefulness and sleep sessions, we imposed a minimum of 30 artifact-free trials for the ECG data analysis and for each condition of interest. Hence, different sets of RR intervals formed the final dataset per participant and consisted of five vigilance states: AWAKE, N1, N2, N3 and REM sleep where available (*Results 1.1. Participants & Suppl. Tables 1 & 2*). One way ANOVAs on RR interval quantities showed no significant differences in trial numbers across auditory conditions within each vigilance state, therefore all RR intervals were included in the statistical analysis. RR intervals for each omission trial order type were averaged for each auditory condition, participant, and each vigilance state.

ECG Statistical Analysis

First, 3x4 repeated measures ANOVAs were performed on the average RR intervals with within-subject factors Auditory Condition (synch, asynch, isoch) and Trial Order (one trial before, trial during, first trial after, second trial after sound omissions) for the wakefulness session and each of the sleep stages (N1, N2, N3, REM) separately. Second, for a sub-set of participants (N=10) who had sufficient trials across wakefulness and all sleep stages, a 5x3x4 repeated measures ANOVA was performed on the average RR intervals with within-subject factors Vigilance State (AWAKE, N1, N2, N3, REM), Auditory Condition (synch, asynch, isoch) and Trial Order (one trial before, trial during, first trial after, second trial after sound omission). Of note, unlike comparisons within vigilance states, trial numbers were matched across vigilance states by randomly selecting a subset of RR intervals based on the minimum number (≥30 trials) of available RR intervals across participants to ensure accurate comparison across vigilance states. Post-hoc t-tests were utilized for pairwise comparisons between all investigated within-subject variables.

Table 2. Hypotheses and Tests performed for the main analyses of the study.

Analysis	Hypothesis	Description	Test
EEG Neural Heartbeat-based Omission Response Analysis	**H1**	**Omission response time-locked to heartbeats during cardio-audio synch but not asynch stimulation in wakefulness and N2 sleep.**	Non-parametric cluster-based permutation statistics comparing synch against asynch, synch against baseline and asynch against baseline for trials time-locked to heartbeat onset for wakefulness and all stages of sleep (N1, N2, N3, REM) separately.
	H0	No omission responses time-locked to heartbeats in all vigilance states.	
EEG Neural Sound-based Omission Response Analysis	**H1**	**Omission response time-locked to the average interstimulus interval during isoch in wakefulness and N2 sleep.**	Non-parametric cluster-based permutation statistics comparing isoch against asynch, isoch against baseline and asynch against baseline for trials time-locked to omission onset for wakefulness and all stages of sleep (N1, N2, N3, REM) separately.
	H0	No omission response time-locked to the average interstimulus interval in all vigilance states.	
SO Analysis	**H1**	**Sound to SO and heartbeat to SO latency differences upon cardio-audio (synch) and Sound to SO latency differences upon audio (isoch) regularity inference compared no regularity conditions (asynch, baseline) in N2 sleep.**	One way repeated measures ANOVAs on the median sound to SO and median heartbeat to SO latency with factor Condition (3 levels: synch, asynch, isoch and 4 levels: synch, asynch, isoch, baseline, respectively).
	H0	No sound to SO and/or heartbeat to SO latency differences across auditory conditions in N2 sleep.	
ECG Cardiac Omission Response	**H1**	**RR intervals in relation to omission onset significantly different across experimental conditions in wakefulness and all stages of sleep.**	3x4 repeated measures ANOVAs on the average RR intervals with factors Auditory Condition (synch, asynch, isoch) and Trial Order (one trial before, trial during, first trial after, second trial after sound omission) for each vigilance state separately (AWAKE, N1, N2, N3, REM). 5x3x4 repeated measures ANOVA on the average RR intervals with factors Vigilance State (AWAKE, N1, N2, N3, REM), Auditory Condition (synch, asynch, isoch) and Trial Order (one trial before, trial during, first trial after, second trial after sound omission).
	H0	No significant differences across experimental conditions independent of vigilance state.	

Data availability

Processed data involved in the analyses for this study will be made available upon publication.

Code availability

EEG data pre-processing and analysis was performed using the MATLAB Tools EEGlab (https://sccn.ucsd.edu/eeglab/index.php) and Fieldtrip (https://www.fieldtriptoolbox.org/) that are publically available. Custom made scripts used to run the analyses in this study will be made available upon publication.

Acknowledgments

We express our gratitude to Nathalie Nguepnjo Nguissi, Elsa Dosi and Diana Ortolani for assistance during data acquisition. We extend our thanks to Dr Aurore Guyon Postalci from SOMNOX for performing the stage scoring of the sleep data. We thank Rupert Ortner and the g.tec team for technical support.

This work was supported by a Spark SNSF Grant (no. 196194) awarded to M.D.L.

Author contributions

A.P., C.P., S.S. and M.D.L. designed the experiment. A.P. conducted the experiment and acquired the data. A.P. and M.D.L. analyzed the data and wrote the manuscript. C.P. and S.S. edited the manuscript.

Declaration of interests

The authors declare that there are no competing interests.

References

Adelhöfer, N., Schreiter, M.L., and Beste, C. (2020). Cardiac cycle gated cognitive-emotional control in superior frontal cortices. Neuroimage *222: 11727*.

Al, E., Iliopoulos, F., Forschack, N., Nierhaus, T., Grund, M., Motyka, P., Gaebler, M., Nikulin, V. V., and Villringer, A. (2020). Heart-brain interactions shape somatosensory perception and evoked potentials. Proc. Natl. Acad. Sci. U. S. A. *117*, 10575–10584.

Andrillon, T., Pressnitzer, D., Léger, D., and Kouider, S. (2017). Formation and suppression of acoustic memories during human sleep. Nat. Commun. *8: 179*.

Banellis, L., and Cruse, D. (2020). Skipping a Beat: Heartbeat-Evoked Potentials Reflect Predictions during Interoceptive-Exteroceptive Integration. Cereb. Cortex Commun. *1*, 1–14.

Barascud, N., Pearce, M.T., Griffiths, T.D., Friston, K.J., and Chait, M. (2016). Brain responses in humans reveal ideal observer-like sensitivity to complex acoustic patterns. Proc. Natl. Acad. Sci. U. S. A. *113*, E616-25.

Bastuji, H., Garcia-Larrea, L., Franc, C., and Mauguiere, F. (1995). Brain Processing of Stimulus Deviance During Slow-Wave and Paradoxical Sleep: A Study of Human Auditory Evoked Responses

using the Oddball Paradigm. J. Clin. Neurophysiol. *12*, 155–167.

Benjamini, Y., and Hochberg, Y. (1995). Controlling the False Discovery Rate: A Practical and Powerful Approach to Multiple Testing. J R Stat. Soc. B *57*, 289–300.

Besedovsky, L., Ngo, H.V. V., Dimitrov, S., Gassenmaier, C., Lehmann, R., and Born, J. (2017). Auditory closed-loop stimulation of EEG slow oscillations strengthens sleep and signs of its immune-supportive function. Nat. Commun. *8: 1984*.

Blanchard, D.C., Griebel, G., Pobbe, R., and Blanchard, R.J. (2011). Risk assessment as an evolved threat detection and analysis process. Neurosci. Biobehav. Rev. *35*, 991–998.

Bouchard, M., Lina, J.M., Gaudreault, P.O., Lafreniret, A., Duba, J., Gosselin, N., and Carrier, J. (2021). Sleeping at the switch. Elife *10*, 1–17.

Chennu, S., Noreika, V., Gueorguiev, D., Shtyrov, Y., Bekinschtein, T.A., and Henson, R. (2016). Silent expectations: Dynamic causal modeling of cortical prediction and attention to sounds that weren't. J. Neurosci. *36*, 8305–8316.

Delorme, A., and Makeig, S. (2004). EEGLAB: An open source toolbox for analysis of single-trial EEG dynamics including independent component analysis. J. Neurosci. Methods *134*, 9–21.

Demarchi, G., Sanchez, G., and Weisz, N. (2019). Automatic and feature-specific prediction-related neural activity in the human auditory system. Nat. Commun. *10: 3440*.

Dercksen, T.T., Widmann, A., Schröger, E., and Wetzel, N. (2020). Omission related brain responses reflect specific and unspecific action-effect couplings. Neuroimage *215: 11684*.

Van Elk, M., Lenggenhager, B., Heydrich, L., and Blanke, O. (2014). Suppression of the auditory N1-component for heartbeat-related sounds reflects interoceptive predictive coding. Biol. Psychol. *99*, 172–182.

Endoh, H., Kamimura, N., Honda, H., and Nitta, M. (2019). Early prognostication of neurological outcome by heart rate variability in adult patients with out-of-hospital sudden cardiac arrest. Crit. Care *23: 323*.

Garrido, M.I., Friston, K.J., Kiebel, S.J., Stephan, K.E., Baldeweg, T., and Kilner, J.M. (2008). The functional anatomy of the MMN: A DCM study of the roving paradigm. Neuroimage *42*, 936–944.

Garrido, M.I., Kilner, J.M., Stephan, K.E., and Friston, K.J. (2009). The mismatch negativity: a review of underlying mechanisms. Clin. Neurophysiol. *120*, 453–463.

Gladwin, T.E., Hashemi, M.M., van Ast, V., and Roelofs, K. (2016). Ready and waiting: Freezing as active action preparation under threat. Neurosci. Lett. *619*, 182–188.

Heilbron, M., and Chait, M. (2018). Great Expectations: Is there Evidence for Predictive Coding in Auditory Cortex? Neuroscience *389*, 54–73.

Hennevin, E., Huetz, C., and Edeline, J.M. (2007). Neural representations during sleep: From sensory processing to memory traces. Neurobiol. Learn. Mem. *87*, 416–440.

Ibáñez, V., Silva, J., and Cauli, O. (2018). A survey on sleep assessment methods. PeerJ *2018*, 1–26.

Iber, C., Ancoli-Israel, S., Chesson Jr., A.L., and Quan, S.F. (2007). The AASM Manual for the Scoring of Sleep and Associated Events.

Jennings, J.R., and Van Der Molen, M.W. (2005). Preparation for speeded action as a psychophysiological concept. Psychol. Bull. *131*, 434–459.

Kimura, K. (2019). Cardiac cycle modulates reward feedback processing: An ERP study. Neurosci. Lett. *711: 13447*.

Kouider, S., Andrillon, T., Barbosa, L.S., Goupil, L., and Bekinschtein, T.A. (2014). Inducing task-relevant responses to speech in the sleeping brain. Curr. Biol. *24*, 2208–2214.

Kunzendorf, S., Klotzsche, F., Akbal, M., Villringer, A., Ohl, S., and Gaebler, M. (2019). Active information sampling varies across the cardiac cycle. Psychophysiology *56: e13322*.

van Laarhoven, T., Stekelenburg, J.J., and Vroomen, J. (2017). Temporal and identity prediction in visual-auditory events: Electrophysiological evidence from stimulus omissions. Brain Res. *1661*, 79–87.

van Laarhoven, T., Stekelenburg, J.J., Eussen, M.L.J.M., and Vroomen, J. (2020). Atypical visual-auditory predictive coding in autism spectrum disorder: Electrophysiological evidence from stimulus omissions. Autism *24*, 1849–1859.

Lecaignard, F., Bertrand, O., Gimenez, G., Mattout, J., and Caclin, A. (2015). Implicit learning of predictable sound sequences modulates human brain responses at different levels of the auditory hierarchy. Front. Hum. Neurosci. *9*, 1–14.

Lechinger, J., Heib, D.P.J., Gruber, W., Schabus, M., and Klimesch, W. (2015). Heartbeat-related EEG amplitude and phase modulations from wakefulness to deep sleep: Interactions with sleep spindles and slow oscillations. Psychophysiology *52*, 1441–1450.

Lojowska, M., Gladwin, T.E., and Roelofs, K. (2015). Supplemental Material for Freezing Promotes Perception of Coarse Visual Features. J. Exp. Psychol. Gen. *144*, 1080–1088.

Maris, E., and Oostenveld, R. (2007). Nonparametric statistical testing of EEG- and MEG-data. J. Neurosci. Methods *164*, 177–190.

Massimini, M., Huber, R., Ferrarelli, F., Hill, S., and Tononi, G. (2004). The sleep slow oscillation as a traveling wave. J. Neurosci. *24*, 6862–6870.

McKenna, J.T., Thankachan, S., Uygun, D.S., Shukla, C., McNally, J.M., Schiffino, F.L., Cordeira, J., Katsuki, F., Zant, J.C., Gamble, M.C., et al. (2020). Basal Forebrain Parvalbumin Neurons Mediate Arousals from Sleep Induced by Hypercarbia or Auditory Stimuli. Curr. Biol. *30*, 2379-2385.e4.

Näätänen, R., Paavilainen, P., Rinne, T., and Alho, K. (2007). The mismatch negativity (MMN) in basic research of central auditory processing: A review. Clin. Neurophysiol. *118*, 2544–2590.

Navarrete, M., Schneider, J., Ngo, H.V. V., Valderrama, M., Casson, A.J., and Lewis, P.A. (2020). Examining the optimal timing for closed-loop auditory stimulation of slow-wave sleep in young and older adults. Sleep *43: 6*, 1–14.

Ngo, H.V. V., Martinetz, T., Born, J., and Mölle, M. (2013). Auditory closed-loop stimulation of the sleep slow oscillation enhances memory. Neuron *78*, 545–553.

Nir, Y., Staba, R.J., Andrillon, T., Vyazovskiy, V. V., Cirelli, C., Fried, I., and Tononi, G. (2011). Regional Slow Waves and Spindles in Human Sleep. Neuron *70*, 153–169.

Nir, Y., Vyazovskiy, V. V., Cirelli, C., Banks, M.I., and Tononi, G. (2015). Auditory responses and stimulus-specific adaptation in rat auditory cortex are preserved across NREM and REM sleep. Cereb. Cortex *25*, 1362–1378.

Nolan, H., Whelan, R., and Reilly, R.B. (2010). FASTER: Fully Automated Statistical Thresholding for EEG artifact Rejection. J. Neurosci. Methods *192*, 152–162.

Ong, J.L., Patanaik, A., Chee, N.I.Y.N., Lee, X.K., Poh, J.H., and Chee, M.W.L. (2018). Auditory stimulation of sleep slow oscillations modulates subsequent memory encoding through altered hippocampal function. Sleep *41: 5*.

Oostenveld, R., Fries, P., Maris, E., and Schoffelen, J.M. (2011). FieldTrip: Open source software for advanced analysis of MEG, EEG, and invasive electrophysiological data. Comput. Intell. Neurosci.

2011: 1568.

Pappens, M., Schroijen, M., Sütterlin, S., Smets, E., Van Den Bergh, O., Thayer, J.F., and Van Diest, I. (2014). Resting heart rate variability predicts safety learning and fear extinction in an interoceptive fear conditioning paradigm. PLoS One *9*.

Park, H.D., and Blanke, O. (2019). Coupling Inner and Outer Body for Self-Consciousness. Trends Cogn. Sci. *23*, 377–388.

Park, H.D., and Tallon-Baudry, C. (2014). The neural subjective frame: From bodily signals to perceptual consciousness. Philos. Trans. R. Soc. B Biol. Sci. *369: 20130*.

Pérez, P., Madsen, J., Banellis, L., Türker, B., Raimondo, F., Perlbarg, V., Valente, M., Niérat, M.C., Puybasset, L., Naccache, L., et al. (2021). Conscious processing of narrative stimuli synchronizes heart rate between individuals. Cell Rep. *36: 109692*.

Perogamvros, L., Park, H.D., Bayer, L., Perrault, A.A., Blanke, O., and Schwartz, S. (2019). Increased heartbeat-evoked potential during REM sleep in nightmare disorder. NeuroImage Clin. *22: 101701*.

Petzschner, F.H., Weber, L.A., Wellstein, K. V., Paolini, G., Do, C.T., and Stephan, K.E. (2019). Focus of attention modulates the heartbeat evoked potential. Neuroimage *186*, 595–606.

Pfeifer, G., Garfinkel, S.N., Gould van Praag, C.D., Sahota, K., Betka, S., and Critchley, H.D. (2017). Feedback from the heart: Emotional learning and memory is controlled by cardiac cycle, interoceptive accuracy and personality. Biol. Psychol. *126*, 19–29.

Pfeiffer, C., and De Lucia, M. (2017). Cardio-audio synchronization drives neural surprise response. Sci. Rep. *7: 14842*.

Raimondo, F., Rohaut, B., Demertzi, A., Valente, M., Engemann, D.A., Salti, M., Fernandez Slezak, D., Naccache, L., and Sitt, J.D. (2017). Brain–heart interactions reveal consciousness in noncommunicating patients. Ann. Neurol. *82*, 578–591.

Recasens, M., and Uhlhaas, P.J. (2017). Test–retest reliability of the magnetic mismatch negativity response to sound duration and omission deviants. Neuroimage *157*, 184–195.

Riganello, F., Zubler, F., Haenggi, M., and De Lucia, M. (2022). Heart rate complexity: An early prognostic marker of patient outcome after cardiac arrest. Clin. Neurophysiol. *134*, 27–33.

Roelofs, K. (2017). Freeze for action: Neurobiological mechanisms in animal and human freezing. Philos. Trans. R. Soc. B Biol. Sci. *372: 20160*.

Ruby, P., Caclin, A., Boulet, S., Delpuech, C., and Morlet, D. (2008). Odd Sound Processing in the Sleeping Brain. J. Cogn. Neurosci. *20*, 296–311.

Sabri, M., Labelle, S., Gosselin, A., and Campbell, K.B. (2002). The effects of digital filtering on mismatch negativity in wakefulness and slow-wave sleep. J. Sleep Res. *11*, 123–127.

Sabri, M., Labelle, S., Gosselin, A., and Campbell, K.B. (2003). Effects of sleep onset on the mismatch negativity (MMN) to frequency deviants using a rapid rate of presentation. Cogn. Brain Res. *17*, 164–176.

Sallinen, M., Kaartinen, J., and Lyytinen, H. (1996). Processing of auditory stimuli during tonic and phasic periods of REM sleep as revealed by event-related brain potentials. J. Sleep Res. *5*, 220–228.

SanMiguel, I., Widmann, A., Bendixen, A., Trujillo-Barreto, N., and Schröger, E. (2013a). Hearing silences: Human auditory processing relies on preactivation of sound-specific brain activity patterns. J. Neurosci. *33*, 8633–8639.

SanMiguel, I., Saupe, K., and Schröger, E. (2013b). I know what is missing here: Electrophysiological prediction error signals elicited by omissions of predicted “what” but not “when.” Front. Hum.

Neurosci. *7: 407*.

Schneider, J., Lewis, P.A., Koester, D., Born, J., and Ngo, H.V. V. (2020). Susceptibility to auditory closed-loop stimulation of sleep slow oscillations changes with age. Sleep *43: 12*.

Schroger, E., and Winkler, I. (1995). Presentation rate and magnitude of stimulus deviance effects on human pre-attentive change detection. Neurosci. Lett. *193*, 185–188.

Sculthorpe, L.D., Ouellet, D.R., and Campbell, K.B. (2009). MMN elicitation during natural sleep to violations of an auditory pattern. Brain Res. *1290*, 52–62.

Sela, Y., Vyazovskiy, V. V., Cirelli, C., Tononi, G., and Nir, Y. (2016). Responses in rat core auditory cortex are preserved during sleep spindle oscillations. Sleep *39: 5*, 1069–1082.

Seligowski, A. V., Reffi, A.N., Phillips, K.A., Orcutt, H.K., Auerbach, R.P., Pizzagalli, D.A., and Ressler, K.J. (2021). Neurophysiological responses to safety signals and the role of cardiac vagal control. Behav. Brain Res. *396*, 112914.

Seth, A.K., Suzuki, K., and Critchley, H.D. (2012). An interoceptive predictive coding model of conscious presence. Front. Psychol. *2: 395*.

Stephan, A.M., Lecci, S., Cataldi, J., and Siclari, F. (2021). Conscious experiences and high-density EEG patterns predicting subjective sleep depth. Curr. Biol. *31*, 5487-5500.e3.

Strauss, M., Sitt, J.D., King, J.R., Elbaz, M., Azizi, L., Buiatti, M., Naccache, L., Van Wassenhove, V., and Dehaene, S. (2015). Disruption of hierarchical predictive coding during sleep. Proc. Natl. Acad. Sci. U. S. A. *112*, E1353–E1362.

Szeska, C., Richter, J., Wendt, J., Weymar, M., and Hamm, A.O. (2021). Attentive immobility in the face of inevitable distal threat—Startle potentiation and fear bradycardia as an index of emotion and attention. Psychophysiology *58*, 1–17.

Todorovic, A., van Ede, F., Maris, E., and de Lange, F.P. (2011). Prior expectation mediates neural adaptation to repeated sounds in the auditory cortex: An MEG study. J. Neurosci. *31*, 9118–9123.

Wacongne, C., Labyt, E., Van Wassenhove, V., Bekinschtein, T., Naccache, L., and Dehaene, S. (2011). Evidence for a hierarchy of predictions and prediction errors in human cortex. Proc. Natl. Acad. Sci. U. S. A. *108*, 20754–20759.

Wacongne, C., Changeux, J.P., and Dehaene, S. (2012). A neuronal model of predictive coding accounting for the mismatch negativity. J. Neurosci. *32*, 3665–3678.

Waselius, T., Wikgren, J., Halkola, H., Penttonen, M., and Nokia, M.S. (2018). Learning by heart: cardiac cycle reveals an effective time window for learning. J Neurophysiol *120*, 830–838.

Winter, O., Kok, A., Kenemans, L., and Elton, M. (1995). Auditory event-related potentials to deviant stimuli during drowsiness and stage 2 sleep. Electroencephalogr. Clin. Neurophysiol. *96*, 398–412.

Zant, J.C., Kim, T., Prokai, L., Szarka, S., McNally, J., McKenna, J.T., Shukla, C., Yang, C., Kalinchuk, A. V., McCarley, R.W., et al. (2016). Cholinergic neurons in the basal forebrain promote wakefulness by actions on neighboring non-cholinergic neurons: An opto-dialysis study. J. Neurosci. *36*, 2057–2067.